

**CHARACTERIZATION OF THE FEMORAL NECK REGION'S RESPONSE TO
THE RAT HINDLIMB UNLOADING MODEL THROUGH TOMOGRAPHIC
SCANNING, MECHANICAL TESTING AND ESTIMATED STRENGTHS**

A Thesis

by

JOSHUA SCOTT KUPKE

Submitted to the Office of Graduate Studies of
Texas A&M University
in partial fulfillment of the requirements for the degree of

MASTER OF SCIENCE

December 2010

Major Subject: Biomedical Engineering

**CHARACTERIZATION OF THE FEMORAL NECK REGION'S RESPONSE TO
THE RAT HINDLIMB UNLOADING MODEL THROUGH TOMOGRAPHIC
SCANNING, MECHANICAL TESTING AND ESTIMATED STRENGTHS**

A Thesis

by

JOSHUA SCOTT KUPKE

Submitted to the Office of Graduate Studies of
Texas A&M University
in partial fulfillment of the requirements for the degree of

MASTER OF SCIENCE

Approved by:

Co-Chairs of Committee,	Harry Hogan
	Susan Bloomfield
Committee Members,	Elizabeth Cosgriff-Hernandez
Head of Department,	Gerald Cote

December 2010

Major Subject: Biomedical Engineering

ABSTRACT

Characterization of the Femoral Neck Region's Reponse to the Rat Hindlimb Unloading Model through Tomographic Scanning, Mechanical Testing and Estimated Strengths. (December 2010)

Joshua Scott Kupke, B.S., The University of Texas at Tyler

Co-Chairs of Advisory Committee: Dr. Harry Hogan
Dr. Susan Bloomfield

Bone quality and the conditions that affect it make up a large field of study. One specific area of interest is the loss in bone strength during exposure to microgravity. The femoral neck (FN) region in particular is an important region of study since a FN failure has such a detrimental effect on mobility. The objective of this study was to characterize the effects of microgravity and recovery on the FN in the adult male hindlimb unloaded (HU) rat model. This was done through peripheral quantitative computed tomography (pQCT), mechanical testing in two different loading conditions, and estimated strength indices.

Adult male Sprague-Dawley rats (6-mo) were grouped into baseline (BL), ambulatory cage control (CC) and hindlimb unloaded (HU); HU and CC animals were further divided into sub-groups (n=15 each): HU euthanized after 28 days of suspension, and HU euthanized after 28, 56, and 84 days of recovery with CC groups being euthanized at each of these time points. The excised right and left

femoral necks were both scanned *ex vivo* using pQCT. Quasi-static mechanical testing was performed with the right femurs positioned vertically and the left femurs positioned laterally at a -10 degree angle. A series of strength indices was used to attempt to predict the mechanical testing results, including a compression index, a bending index and an alternative combination of the two.

HU exposure led to 6.3% lower bone mineral content (BMC), compared to BL and 7.8% lower total volumetric bone mineral density (vBMD) at the FN. The vertical or axial loading showed a 17.1% drop in mechanical strength due to HU exposure. The lateral loading test revealed a 5.4% drop in strength, showing that HU had a greater effect on the axial loading configuration. Also, after just 28 days of recovery, the axial loading test revealed a complete recovery of strength.

None of the strength indexes completely predicted the mechanical behavior of the FN. In the right femur, the combined index had the highest correlation with an R value of 0.94. The bending strength index had the highest correlation in the left lateral testing with an R value of 0.98. However, in all the cases, the strength indexes failed to predict the mechanical behavior at all the time points. In general, the strength indexes provide valuable input, but fail to replace mechanical testing.

DEDICATION

This thesis is dedicated to:

My fiancé, Krystal, for her love, support, and ability to put up with me

My sons, Skyler and Justin, for being the best distractions one could hope

to have

The rest of my family, for the encouragement and support provided

throughout the years.

ACKNOWLEDGMENTS

First, I would like to thank Dr. Hogan for the chance to work under him in the Bone Biomechanics Lab. I would also like to thank my colleagues in the Bone Biomechanics Lab for all the assistance in the overall study and my thesis in particular.

I'd also like to thank Dr. Sue Bloomfield and the personnel of the Bone Biology Lab. They provided assistance in animal care, sample preparation, and pQCT scanning. Particularly, I'd like to express gratitude to Dr. Elizabeth Greene for help in both pQCT and statistical analysis.

NOMENCLATURE

BMC	Bone Mineral Content
vBMD	volumetric Bone Mineral Density
FEA	Finite Element Analysis
FN	Femoral Neck
HU	Hindlimb Unloaded
MNSC	Minimum Neck Cross-Sectional Area
NBSI	Neck Bending Strength Index
NCSI	Neck Compressive Strength Index
PBS	Phosphate Buffered Saline
pQCT	Peripheral Quantitative Computed Tomography
R	Correlation Coefficient
R ²	Coefficient of Determination
SI	Strength Index

TABLE OF CONTENTS

	Page
ABSTRACT	iii
DEDICATION	v
ACKNOWLEDGMENTS	vi
NOMENCLATURE	vii
TABLE OF CONTENTS	viii
LIST OF FIGURES	x
LIST OF TABLES	xiv
1. INTRODUCTION	1
1.1 Problem	1
1.2 Objectives	3
1.3 Overview	5
2. BACKGROUND	6
2.1 General Bone Structure	6
2.2 The Femoral Neck Region	7
2.3 The Hindlimb Unloaded (HU) Model	10
2.4 Radiographic Tomography	11
2.5 Mechanical Testing	11
2.6 Strength Indices	13
3. METHODS	15
3.1 Overall Study Design	15
3.2 pQCT Scans and Analysis	17
3.3 Femoral Neck Testing	19
3.4 Estimated Strength	24
3.5 Statistical Methods	26
4. RESULTS	28

	Page
4.1 pQCT Data	28
4.2 Femoral Neck Testing Axial Loading Configuration	33
4.3 Femoral Neck Testing Lateral Loading Configuration	35
4.4 Loading Comparisons	37
4.5 Strength Indices	40
4.5.1 Axial Strength Indices	40
4.5.2 Lateral Strength Indices	46
5. DISCUSSION AND SUMMARY	52
5.1 pQCT Data	52
5.2 Axial Testing	57
5.3 Lateral Testing	59
5.4 Comparison of Axial and Lateral Testing (HU Effect)	60
5.5 Strength Index Correlations	63
5.6 Limitations	65
5.7 Summary	65
6. FUTURE WORK	67
6.1 Test Fixture Refinements	67
6.2 New Strength Index Approach	67
6.3 Repeatability Studies	68
6.4 Finite Element Analysis	68
REFERENCES	70
APPENDIX A	74
APPENDIX B	79
APPENDIX C	89
APPENDIX D	92
APPENDIX E	99
VITA	102

LIST OF FIGURES

	Page
Figure 1: General bone structure.....	6
Figure 2: Proximal femur	8
Figure 3: Comparison of the femoral neck region in humans and rats	9
Figure 4: Femoral neck loading configurations. (B) Axial Loading in a standing fixture. (A) Lateral Loading in a clamp system.	12
Figure 5: Schematic depiction of study design showing groups and end points for each.....	16
Figure 6: Representative pQCT scans of a right femoral neck (A, B, C). Sample cross-sectional scans (D) Scout view with the three lines indicating the positions of the cross-sectional scans. (E). The schematic cross-section indicated the definitions of the total, cortical, and trabecular regions. The area of the trabecular compartment is termed the marrow area.....	18
Figure 7: (A) Axial loading fixture consisting of supporting plate on an Instron 3345 testing frame. (B) Schematic of axial loading test configuration.....	20
Figure 8: Solid model of fixture for holding femoral neck for testing in the lateral direction	21

	Page
Figure 9: (A) Photograph showing a specimen in the test machine for the lateral loading configuration. (B) Schematic of lateral loading test configuration.....	22
Figure 10: Photograph showing a close-up view of a specimen in the fixture for the lateral loading configuration. Bone shaft is stabilized between rubber lined compression plates.	23
Figure 11: Loading vectors, relevant angles and example force components ..	26
Figure 12: Weekly body mass data of combined hindlimb unloaded (HU) groups and combined cage control (CC) groups	28
Figure 13: Percent change in total bone mineral content (BMC) in femoral neck after 28 days of hindlimb unloading (HU). CC = cage controls.....	31
Figure 14: Percent change in total volumetric bone mineral density (vBMD) in femoral neck after 28 days of hindlimb unloading (HU). CC = cage controls	31
Figure 15: Maximum load sustained during FN testing for axial loading case ..	34
Figure 16: Stiffness of linear region during FN testing for axial loading case ...	35
Figure 17: Maximum load sustained during FN testing for lateral loading case.....	36
Figure 18: Stiffness of linear region during FN testing for lateral loading case.....	37

Figure 19: Loading comparisons of maximum loads sustained graphed as percent change from baseline	39
Figure 20: Loading comparisons of maximum loads sustained graphed as force vs. time point during study.	39
Figure 21: Neck Compression Strength Index (NCSI) calculated from right leg compared to the maximum load sustained during axial testing..	41
Figure 22: Neck Bending Strength Index (NBSI) calculated from right leg compared to the maximum load sustained during axial testing	42
Figure 23: Combined Existing Strength Indices calculated from right leg compared to the maximum load sustained during axial testing	42
Figure 24: Adjusted Neck Compression Strength Index (adjNCSI) calculated from right leg compared to the maximum load sustained during axial testing.....	43
Figure 25: Adjusted Neck Bending Strength Index (adjNBSI) calculated from right leg compared to the maximum load sustained during axial testing.....	43
Figure 26: Combined Adjusted Strength Indices calculated from right leg compared to the maximum load sustained during axial testing	44
Figure 27: Neck Compressive Strength Index (NCSI) calculated from left leg compared to the maximum load sustained during lateral testing	47

Figure 28: Neck Bending Strength Index (NBSI) calculated from left leg compared to the maximum load sustained during lateral testing	48
Figure 29: Combined Existing Strength Index calculated from left leg compared to the maximum load sustained during lateral testing	48
Figure 30: Adjusted Neck Compressive Strength Index (adjNCSI) calculated from left leg compared to the maximum load sustained during lateral testing	49
Figure 31: Adjusted Neck Bending Strength Index (adjNBSI) calculated from left leg compared to the maximum load sustained during lateral testing	49
Figure 32: Combined Adjusted Strength Index calculated from left leg compared to the maximum load sustained during lateral testing	50

LIST OF TABLES

	Page
Table 1: Femoral Neck Bone Mineral Content (BMC) and Volumetric Bone Mineral Density (vBMD) after 28 Days of Unloading and through 84 Days of Recovery	30
Table 2: Geometric Parameters from pQCT Scans of Right Femur	32
Table 3: Axial Loading FN Test Mechanical Properties	34
Table 4: Lateral Loading FN Test Mechanical Properties	36
Table 5: Comparison of Maximum Load for FN Mechanical Testing in the Two Loading Configurations: Axial and Lateral	38
Table 6: Axial Strength Indices	41
Table 7: Strength Index Correlation for Axial Test	46
Table 8: Lateral Strength Indices	47
Table 9: Strength Index Correlation for Lateral Test	51

1. INTRODUCTION

1.1 Problem

The proximal femur region, specifically the femoral neck, forms a critical part of the acetabulofemoral joint, or hip joint. A number of forces are applied to this region due to the variability of the loading conditions to which it is subjected. Because of the variety of loading conditions, the femoral neck is an essential structure in the mobility of the lower limbs.

There are many environments and medical conditions which have negative effects on general bone mineralization and morphology. Microgravity exposure has been shown to have harmful effects on many facets of bone quality.⁽¹⁾ Morphology is affected on many levels from the micro architecture of trabeculae, to the overall cross-sectional geometry of bones. Bone mineralization is also adversely affected, with both bone mineral density (BMD) and overall bone mineral content (BMC) experiencing significant declines.

Various medical conditions can also affect the quality of bone. Osteoporosis is a medical condition in which an individual's BMD is considerably lower than the norm for their respective age group. Elderly persons frequently suffer from this condition.

Because of the relatively high forces to which the femoral neck is

⁽¹⁾ This thesis follows the style of the Journal of Bone and Mineral Research.

subjected, many of the individuals suffering from a debilitating bone condition experience fractures in this region. BMD is often used as an indicator of bone quality and bone strength. However BMD does not always tell the whole story. It is important to more thoroughly study the effects changes in these parameters have on bone strength.

One area of interest is the effects of microgravity on the human skeleton. Microgravity exposure poses a serious risk for a number of reasons. The drastic effect that unloading has on bone mineralization and morphology can have a serious effect on bone strength.⁽¹⁾ Also because of the strenuous nature of the tasks and responsibilities of men and women during spaceflight, especially during extravehicular activities, a fracture could have much more serious repercussions. The risk is compounded by the lack of advanced medical attention due to the isolation of spaceflight. The complete characterization of the effects of microgravity exposure and reloading of bone after weight is restored, is very important.

Animal models are frequently used as analogues due to a number of reasons. A much larger degree of control is possible as opposed to human studies which utilize astronaut subjects. These areas of control include the length of unloading, which can be more tightly controlled, as can the timing of further testing during reloading. Also it is much easier to obtain a large sample size, giving any results greater statistical significance.

One very important advantage of animal based studies is the ability to perform both radiographic scans and destructive mechanical testing on bone from test subjects. This is important because it provides an opportunity to correlate radiographic parameters to strength values obtained from mechanical testing. More specifically, the femoral neck has not been studied as extensively as other anatomic sites in previous research utilizing the adult rat hindlimb unloading (HU) model. Therefore, obtaining detailed loss and recovery data for the femoral neck will provide new data and insights. The primary objective of this study is thus to characterize the effects of unloading and varying periods of reloading on the femoral neck region in an animal model of microgravity. This will be done both with non destructive radiographic scans and destructive mechanical testing. Analysis from scan data will then be correlated and refined so as to provide a better estimation of true mechanical strength. These objectives are explained in detail in the following section.

1.2 Objectives

The detailed objectives of this thesis are as follows:

1. To comprehensively characterize the effects of microgravity exposure and varying periods of recovery through reloading on the femoral neck region through peripheral quantitative computed tomography (pQCT) scans.

Specifically, this will be accomplished by examining BMC and vBMD over

the total cross-section, in the cortical compartment, and in the cancellous compartment.

2. To comprehensively characterize the effects of microgravity exposure and varying periods of recovery through reloading on the femoral neck region through mechanical testing of the femoral neck region in two different loading configurations. This will be accomplished by taking groups of specimens immediately after unloading and after varying periods of reloading and subjecting the femoral neck region to a compression-bending-shear test. These tests will be performed in two different configurations. The first configuration is upright and loaded parallel to the axis of the femoral shaft, and this is termed “axial” loading in this thesis. The second loading configuration will be produced laterally with the load applied at an angle to the femoral shaft axis, and this is termed “lateral” loading in this thesis.
3. To compare the structural mechanical properties of the femoral neck region for axial and lateral loading and how they are affected by hindlimb unloading and recovery.
4. To determine the strength of correlations between the various pQCT parameters under study and mechanical properties.
5. To compare existing estimated strengths based upon pQCT parameters with tested mechanical strengths. Also to develop alternative indices

based upon current strength indices and compare these indices with tested mechanical strengths

1.3 Overview

The body of this thesis is organized into five sections. The next section provides a background over general bone structure, the femoral neck region, the hind limb unloaded rat model, pQCT scans and mechanical testing. Following the background is a methods section describing the procedure for the experiment including the animal study, specimen preparation, pQCT scanning, mechanical testing, and the analysis. The next section is a discussion of the results from the experiment. Finally, a section describing the future work necessary and possible in this area will be presented.

2. BACKGROUND

2.1 General Bone Structure

Bones are made up of a very heterogeneous organic composite. This composite is a rigid type of connective tissue. The tissue in bones can be classified as one of two types, as can be seen in Figure 1. A very compact dense type of bone called cortical, or compact, bone, and a less dense porous type of bone called cancellous, or spongy, bone. Long bones, as the femur is classified, are characterized by a long narrow region known as the diaphysis, which becomes the metaphysis and then the epiphysis at each end

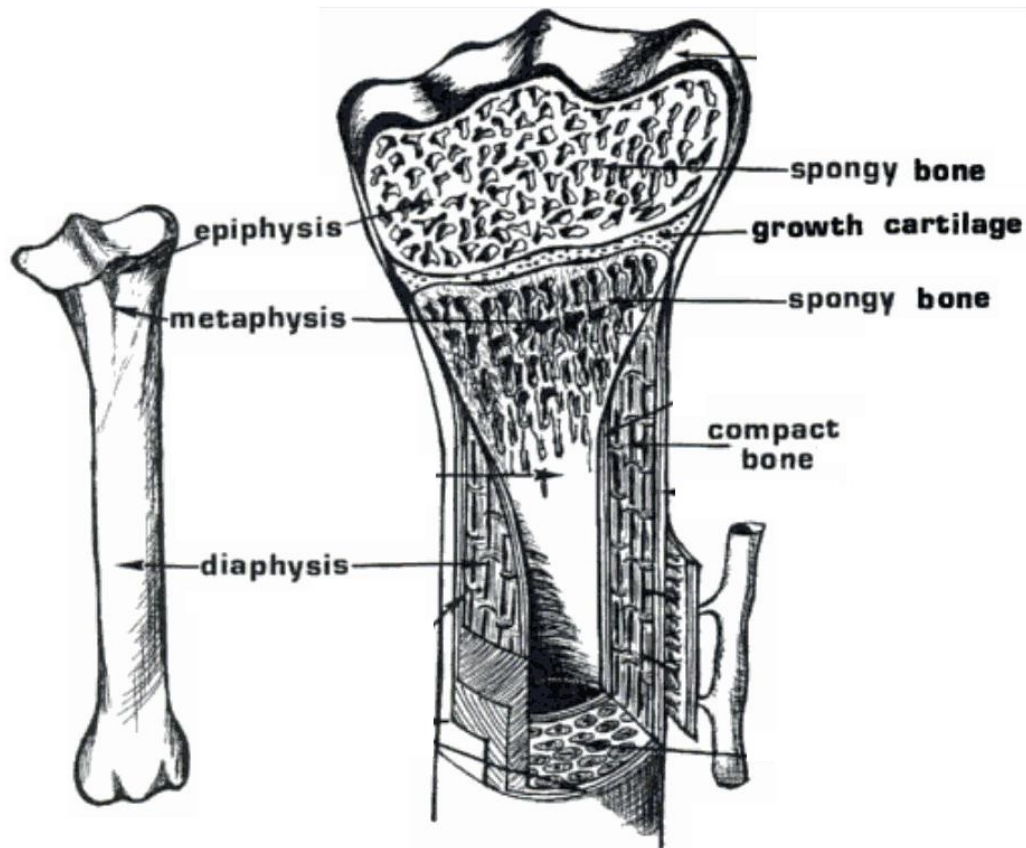


Figure 1: General bone structure [after reference (2)].

Bones have four main functions in the body. The first is that they provide structural support for the body. The second function being that they facilitate movement by providing attachment points and leverage for muscles. The third function is protection. Bones shield many vital organs, examples being the skull protecting the brain and the rib cage protecting the heart and lungs. The fourth function is their ion storage capacity, namely calcium. In this, bones function as a bank of excess ions which can be released to help muscle function and fluid balance. ⁽³⁾

It is their function of support that determines bone's strength. Bone tissue has the ability to adapt to the loads which it must support. This functional adaptation is the result of mechanotransduction in the bone tissue and is known as Wolff's Law. ⁽⁴⁾ The result of Wolff's Law is that each bone in the body has a unique structure suited towards its particular function and loading condition.

2.2 The Femoral Neck Region

The femur is the longest and strongest bone in the human body. With the exception of the clavicle, it is the first bone to show signs of ossification. ⁽⁵⁾

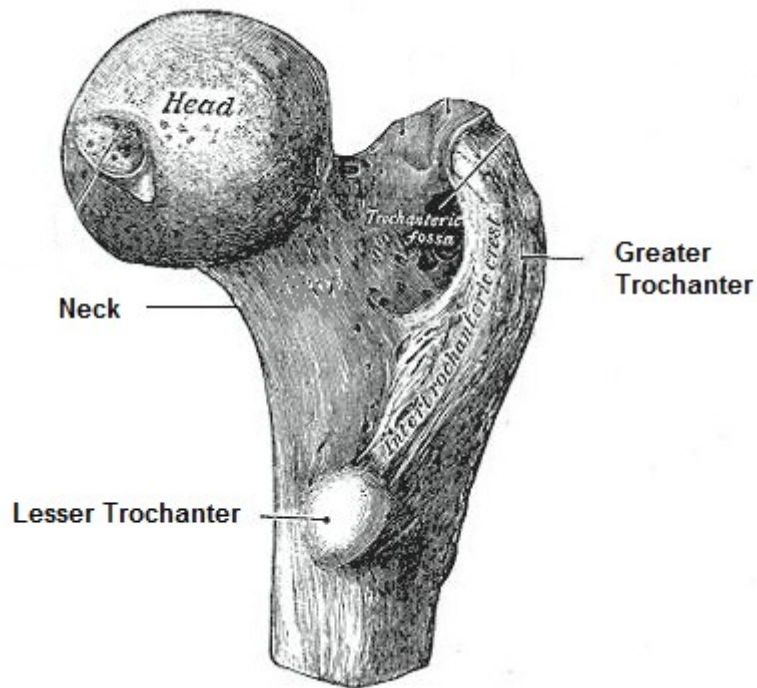


Figure 2: Proximal femur [after reference (5)].

As with other long bones, the femur is made up of the diaphysis and two extremities consisting of a metaphysis region and the epiphysis. The proximal end of the femur, illustrated in figure 2, primarily consists of the femoral head, neck, greater trochanter and lesser trochanter. The head of the femur forms a partial sphere and attaches to the neck which curves downward and joins the femur around the lesser trochanter. The greater trochanter is a protuberance which extends laterally from the proximal end of the femur. While there is variation among species, most walking vertebrates exhibit femurs with these features.

The femoral neck region contains both cortical and cancellous bone. As can be concluded from Wolff's Law, the structure of the femoral neck is adapted to support the particular loads to which it is subjected. Due to this fact, the femoral neck structure is anisotropic and will behave differently depending upon how it is loaded. The loadings which the femoral neck is subjected to are diverse. The femoral neck regularly experiences a very complex stress state. ⁽⁶⁾

It is important to note that there are differences between the human and rat femoral neck region. Figure 3 illustrates the differences in the anatomical features between the two species. As can be seen in Figure 3 the rat has a longer more cylindrical femoral neck. Also the cortical shell is substantially thicker in the rat compared to the human.

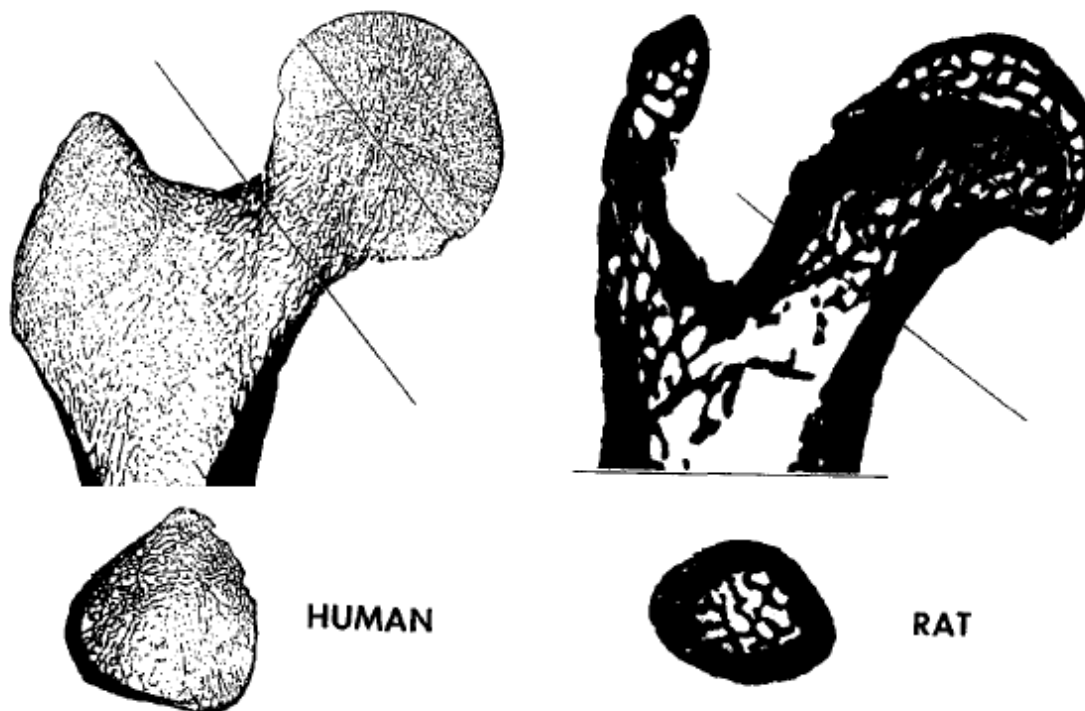


Figure 3: Comparison of the femoral neck region in humans and rats [after reference (7)].

2.3 The Hindlimb Unloaded (HU) Model

In this study the hindlimb unloaded (HU) rat model was used to simulate microgravity exposure. Hindlimb unloading has long served as a well validated model for the musculoskeletal effects experienced during spaceflight. ⁽⁸⁾⁽⁹⁾ There are four important aspects of the HU rat model which make it a valuable predictor for bone response in spaceflight. ⁽⁸⁾

- The model produces musculoskeletal changes similar to those experienced during spaceflight.
- The model allows unrestrictive movement of all limbs while being unloaded just as in spaceflight.
- The model does not produce inordinate amounts of stress in the test animals, as shown by maintenance of body weight similar to control animals. This is generally shown by comparing body mass data between HU and control groups
- The model causes a cephalic fluid shift similar to that observed during spaceflight.

Since the HU rat model has proven to accurately predict bone response to microgravity in many studies ⁽⁸⁾⁽⁹⁾ as well as in our own lab ⁽¹⁰⁾, it was chosen for this study.

2.4 Radiographic Tomography

Three dimensional x-ray imaging, one of the most widely used diagnostic procedures, can provide insight into bone conditions. Quantitative computed tomography, using a series of two dimensional x-ray images rotated around an axis, can provide geometric properties of bones as well as densitometric properties. Peripheral quantitative computed tomography (pQCT) is a specific type of quantitative computed tomography developed for use in human wrist or tibia and in research animals.

Using the properties obtained from these scans, it is possible to gain understanding of changes in bone mineral content (BMC) and volumetric bone mineral density (vBMD). Also geometric parameters, such as area and polar moment of inertia, may be assessed. While pQCT scans do not completely portray the biomechanical strength of bone, they do provide a non-destructive, non-invasive approach to analyzing bone and can be performed on a live animal multiple times, providing longitudinal data.

2.5 Mechanical Testing

Having both cortical and trabecular compartments, the femoral neck is a useful site to test unloading effects on both bone types. Femoral neck testing has been used in hindlimb unloading studies ^{(10) (11) (12)} as well as rat studies involving estrogen deficiency, ^{(13) (14)} and diet, exercise and diabetes. ^{(15) (16) (17)}

⁽¹⁸⁾ These various studies found that femoral neck strength declines significantly with disuse, estrogen deficiency, and diabetes.

The primary method of testing the mechanical strength of the femoral neck is the femoral neck compression test. As mentioned previously, the strength of the femoral neck region depends upon the loading vector. Figure 4 illustrates two such loading configurations. Figure 4a shows loading in an axial, or weight bearing, configuration. Figure 4b illustrates loading in a lateral, or fall, configuration.

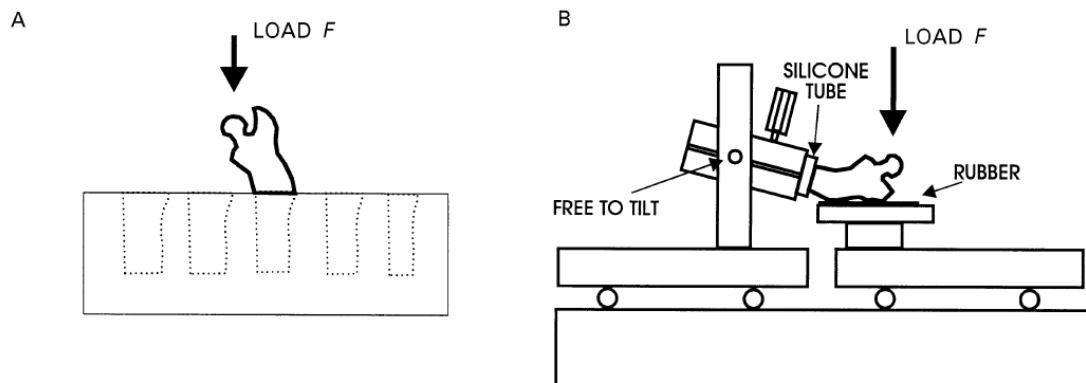


Figure 4: Femoral neck loading configurations [after reference (19)]. (A) Axial loading in a standing fixture. (B) Lateral loading in a clamp system.

All of the studies mentioned previously utilized the axial loading configuration. The lateral loading configuration has been used primarily in human cadaver studies, since it approximates the loading encountered during a fall to the side in bipeds. ^{(20) (21)} Jamsa et al. has compared femoral neck strength data derived from the axial and lateral loading configurations in mouse studies. ^{(19) (22)} Zhang et al. has used the two loading configurations to examine

the effects of ovariectomy on the strength of the femoral neck in different loading vectors.⁽²³⁾

In this test, in either configuration, a load is applied quasi-statically until fracture occurs. These tests produce a combination of multiple stress conditions including compression, bending and shear. This complex loading leads to irregular fracture cross-sections. This makes the calculation of intrinsic material properties unreliable. For this reason only structural properties are normally reported from femoral neck tests. This complex stress state also makes three dimensional modeling difficult.

2.6 Strength Indices

While pQCT scans provide geometric and densitometric information about bone, these parameters cannot accurately predict the mechanical strength of a bone. Jarvinen et al. attempted to predict femoral neck strength similarly using densitometric parameters obtained from dual-energy x-ray absorptiometry (DXA) scans.⁽²⁴⁾ None of the parameters fully explained the mechanical tests. Pulkkinen et al. combined these DXA parameters with geometric properties for some improvement.⁽²⁵⁾

Strength indices also use multiple parameters from scan analysis to estimate how much a particular region of bone will withstand a certain type of stress. Lang et al. has used a neck compression strength index (NCSI) and a neck bending strength index (NBSI) to estimate the strength of the femoral neck

in astronauts before mission, immediately after mission and after a period of recovery.⁽²⁶⁾

$$NCSI = iBMD^2 * MNCS \quad (1)$$

$$NBSI = \frac{I_x + I_y}{W} \quad (2)$$

NCSI (Equation 1) takes into account the total BMD of the region and the minimum cross-sectional area. As shown in Equation 2, the NBSI uses I_x , which is the modulus weighted cross-sectional moment of inertia in the x direction, and I_y , which is the modulus weighted cross-sectional moment of inertia in the y direction. The modulus is estimated using an algorithm based on the BMD. The combination of these two terms is divided by the bone width of the minimum cross-sectional area W.

Bending strength index has been used in rats to estimate the mechanical strength of rat bones during three point bending tests at the femur diaphysis.⁽²⁷⁾ This study found that the strength index had a much higher correlation with mechanical strength than either BMD or CSMI independently.

3. METHODS

3.1 Overall Study Design

This study was carried in the Bone Biomechanics Laboratory in the Department of Mechanical Engineering and in the Bone Biology in the Department of Health and Kinesiology. The purpose of the study was to examine key aspects of bone quality as it recovers from changes induced by hindlimb unloading. This was done through the use of pQCT scans and mechanical strength from mechanical testing. This thesis focuses on the femoral neck in particular.

In this study, six month old male Sprague Dawley rats were subjected to hindlimb unloading. Animals were separated into nine groups of fifteen. One group of animals was sacrificed at the beginning of the study. (baseline group) Four groups of animals were unloaded using the HU model. These groups included a hindlimb unloaded group (HU) which was sacrificed immediately after unloading, a 28-day recovery group (REC28), a 56-day recovery group (REC56), and an 84-day recovery group (REC84). Four groups of animals were used as ambulatory cage controls in order to obtain age-matched comparisons for each of the unloaded groups. These groups include cage control groups sacrificed at 28, 56, 84 and 112 days (CC28, CC56, CC84, and CC112). Figure 5 illustrates the groupings of the study.

Animal Age	6 Months	7 Months	8 Months	9 Months	10 Months
Day of Study	Day 0	Day 28	Day 56	Day 84	Day 112
Baseline (n=15)					
HU only					
CC28 (n=15)					
HU (n=15)	Hindlimb Unloading				
HU + 1 Recovery					
CC56 (n=15)					
REC28 (n=15)	Hindlimb Unloading	28d Recovery			
HU + 2 Recovery					
CC84 (n=15)					
REC56 (n=15)	Hindlimb Unloading	56d Recovery			
HU + 3 Recovery					
CC112 (n=15)					
REC84 (n=15)	Hindlimb Unloading	84d Recovery			

Figure 5: Schematic depiction of study design showing groups and end points for each.

Animals were acclimated for two weeks, in single housing prior to unloading. All animals remained singly housed for the duration of the study. A modification of the Morey-Holton method of HU was used to unload the animals. ⁽⁹⁾ The animals were anesthetized and two strips of cloth tape were attached to the lateral sides of the tail using a cyanoacrylate adhesive. These strips are attached to a fish hook and wire. After the adhesive is allowed to dry, the animal is awakened and the tail harness is attached to a wire spanning the top of the cage. The hind limbs were allowed to bear weight for 24 hours to allow the animal to recover from anesthesia. This allows the animals to adapt to the anesthesia and tail harness. During this period animals generally resume normal feeding and grooming behaviors. After this recovery, the animals are suspended by their tail high enough to lift the hind quarters and prohibit any weight bearing on the hind limbs for the 28 days of unloading. During the first week of

unloading, the daily food intake of the suspended animals is measured. The average consumption per animal is calculated for the suspended animals and the cage control animals' food is restricted to this average. This pair feeding ensures that the animals are taking in the same amount of food. Animals were weighed weekly.

After the animals were sacrificed, the right femur was excised and cut in half. The proximal half was wrapped in gauze soaked in phosphate buffered saline (PBS) and stored frozen at -20°C. The entire left femur was excised and stored in a similar fashion. Each left femur was subsequently subjected to three-point bending mechanical testing, and the proximal half was stored separately for this study. The bones were kept frozen and only allowed to reach room temperature when scans or mechanical testing was performed.

3.2 pQCT Scans and Analysis

Tomographic scans were performed *ex vivo* on the right and left femoral necks using a Stratec XCT Research-M device (Norland Corp., Fort Atkinson, WI). Daily calibration of this machine was performed using a hydroxyapatite cone phantom to ensure precision. A voxel size of .071 x .071 x .5 mm was used, and the scan speed was 2.5 mm/s.

The proximal half of the femurs were carefully placed in a mold designed to hold the femoral neck in alignment with the scanning axis of the CT scanner.

⁽¹⁰⁾⁽²⁸⁾ Right femurs were cut during tissue collection as mentioned previously

and left femurs were broken in three point bending tests prior to scanning. The proximal femurs were wrapped in PBS soaked gauze to ensure the bones remained hydrated throughout the scanning process. A scout view scan was performed and three adjacent scans were made of the femoral neck just below the femoral head. Slices were placed with centers 0.5 millimeters apart resulting in a total length of 1.5 millimeters being scanned. Figure 6 depicts representative images of the three slices obtained and a scout view from one of the specimens, and some of the terminology used for cross-sectional parameters.

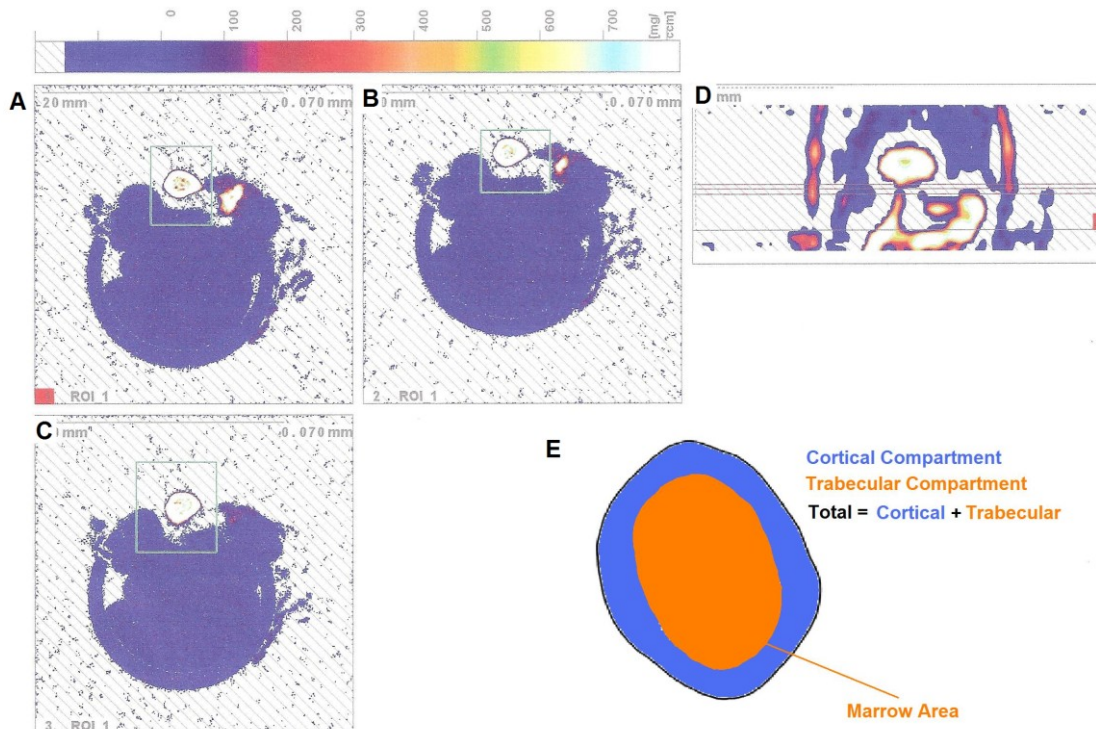


Figure 6: Representative pQCT scans of a right femoral neck (A, B, C). Sample cross-sectional scans (D) Scout view with the three lines indicating the positions of the cross-sectional scans. (E). The schematic cross-section indicated the definitions of the total, cortical, and trabecular regions. The area of the trabecular compartment is termed the marrow area.

The scan slices were analyzed using Stratec software (version 6.00, Norland Corp., Fort Atkinson, WI). The parameters used in this study were obtained using the cancellous bone density analysis (CALCBD) with contour mode 1, peel mode 1 with a threshold value of 280 mg/cm³.

3.3 Femoral Neck Testing

The femoral necks were subjected to mechanical testing to failure. Tests were performed on an Instron 3345. A quasistatic load was applied in displacement control at 2.54 mm/min. The applied force was measured with a 1000 N load cell. Displacement was measured internally by the machine cross head's position. Force and displacement data were collected by Bluehill software (version 2.14.582, Instron Bluehill) at 10Hz.

Two different loading configurations were used to determine the mechanical strength. The right proximal femurs were placed up right with the diaphysis portion of the bone supported in a metal frame. A photograph of the fixture for this test is illustrated in Figure 7 along with a schematic showing the test configuration.

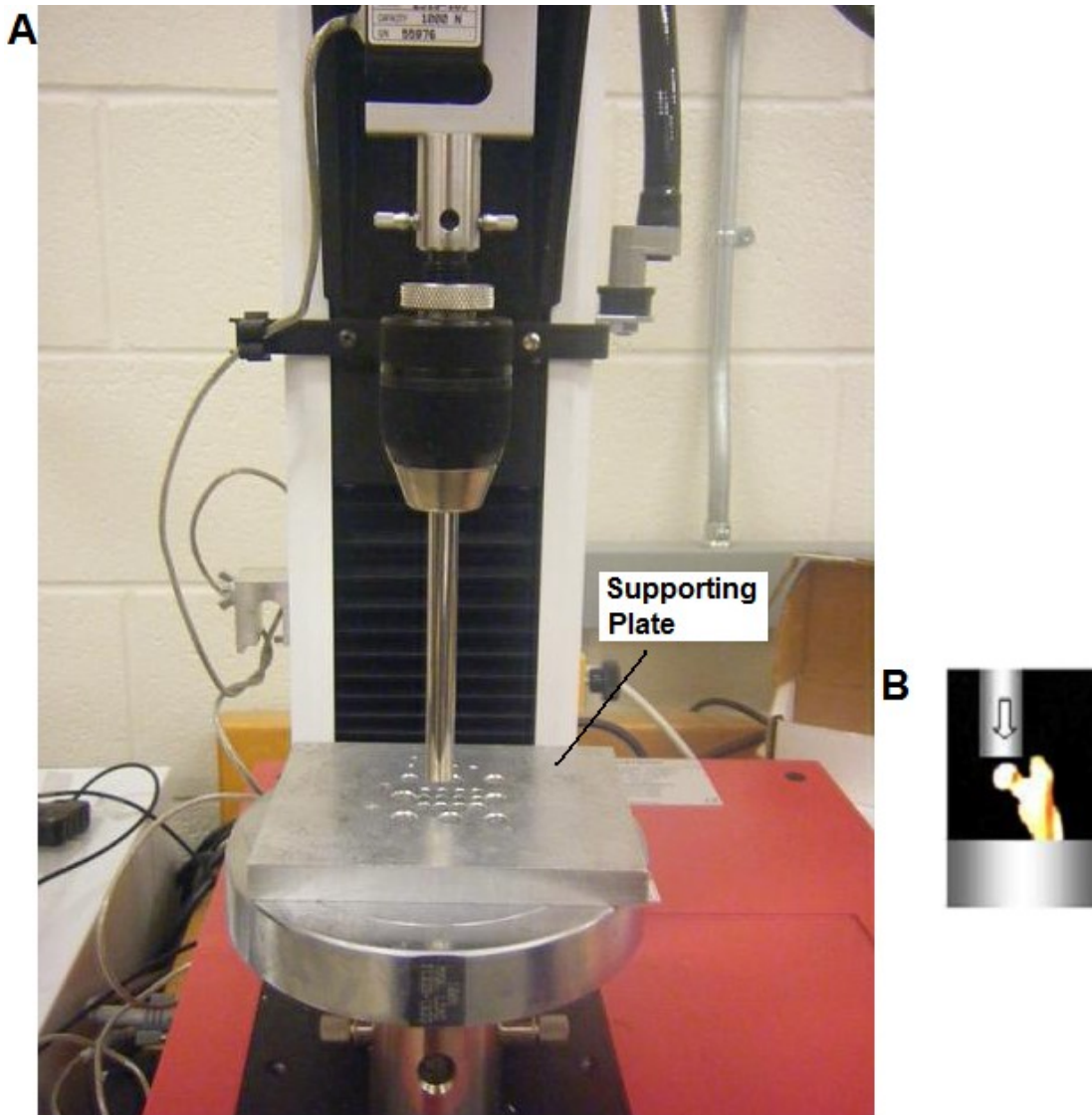


Figure 7: (A) Axial loading fixture consisting of supporting plate on an Instron 3345 testing frame. (B) Schematic of axial loading test configuration.

A 10 mm cylindrical platen with a flat head was used to apply a load to the femoral head, parallel to the axis of the shaft of the femur. This loading simulates a loading such as that experienced by the femoral neck in humans during an upright, one-legged stance.

The second loading configuration was achieved by designing a fixture that supports the proximal femur “laying down” with the shaft of the femur rotated approximately 100 degrees from vertical. Figure 8 illustrates the solid model assembly of the fixture fabricated for this testing configuration. Appendix A contains complete drawings of the fixture design.

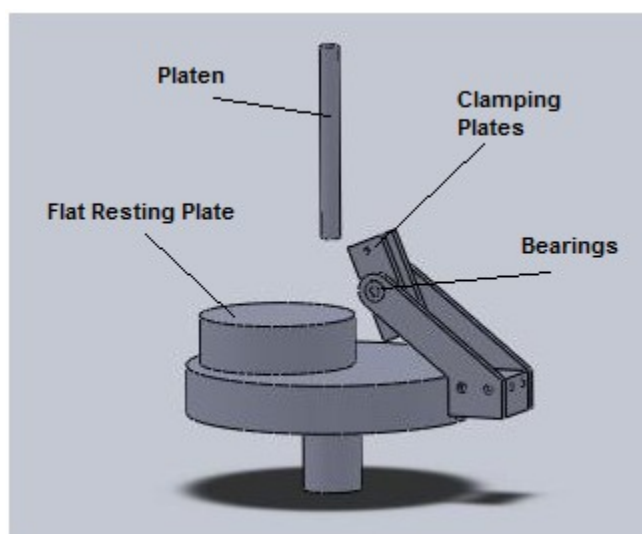


Figure 8: Solid model of fixture for holding femoral neck for testing in the lateral direction.

This setup was used to test the mechanical strength of the left femoral necks. In this configuration a 10 mm cylindrical platen applies a load to the femoral head while the greater trochanter rests on a flat plate situated beneath the fixture. The diaphysis portion of the femur is clamped between two plates fitted with rubber supports in order to support the proximal femur at the appropriate 10 degree angle as performed in previous studies.^{(19) (20) (21) (22)} The femur is supported by a pair of bearings so that no moment is applied to the

diaphysis region. Figures 9 and 10 show the test being performed on one of the left proximal femurs. This 10 degree angle created with the surface the bone is resting on and the shaft of the femur approximates the angle of the human femur to the ground during a lateral fall. This simulates the lateral loading applied to the femoral neck during a fall in humans.

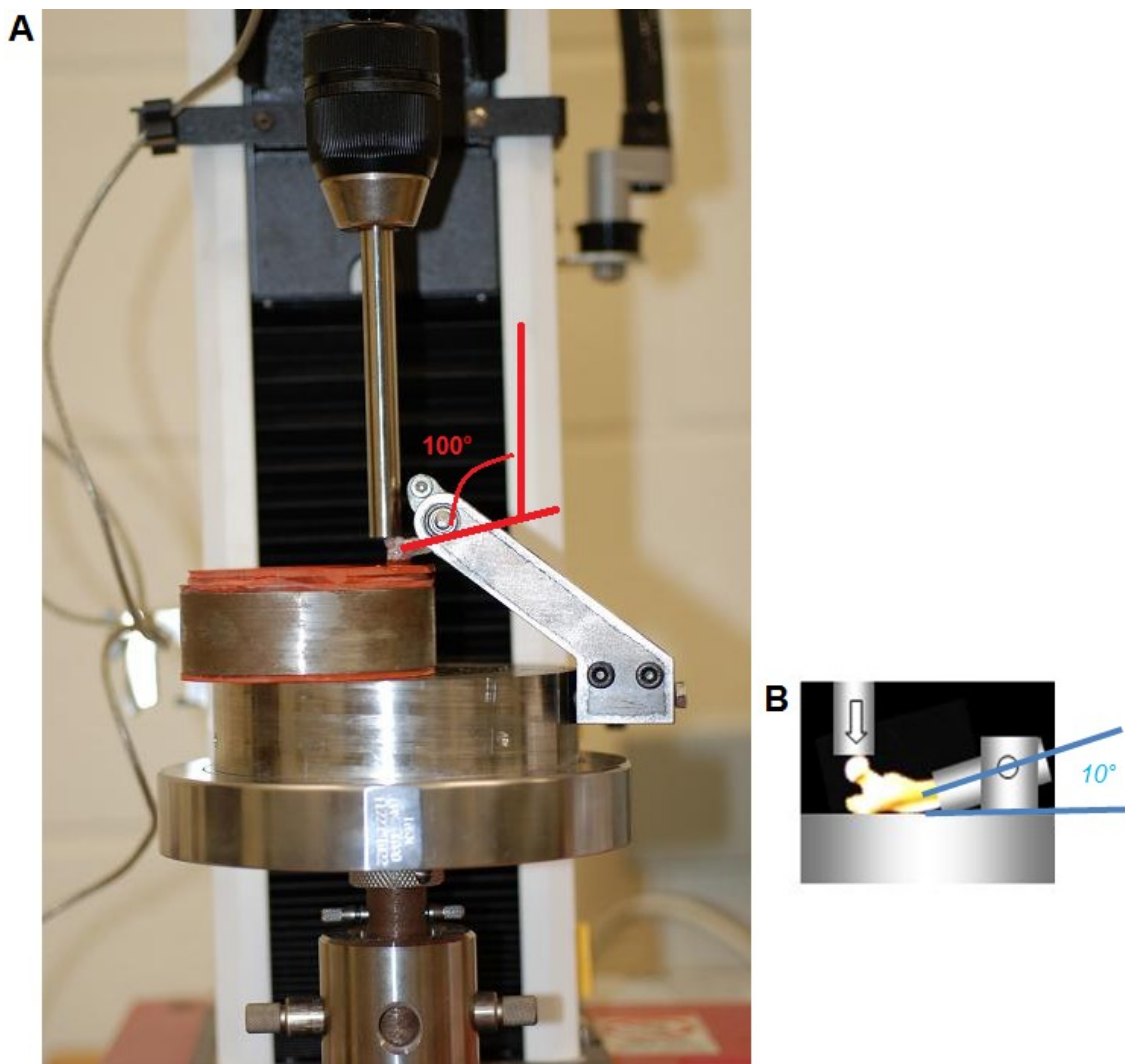


Figure 9: (A) Photograph showing a specimen in the test machine for the lateral loading configuration. (B) Schematic of lateral loading test configuration.

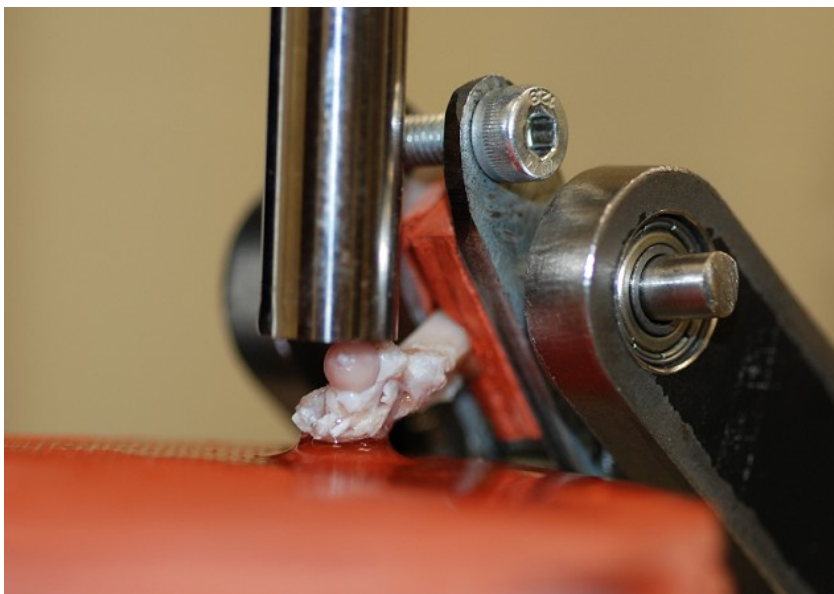


Figure 10: Photograph showing a close-up view of a specimen in the fixture for the lateral loading configuration. Bone shaft is stabilized between rubber lined compression plates.

In both of these loading configurations, the distal end of the proximal end was not treated in any way (e.g. fixing or potting in a substrate material) in order to stabilize the bone during the testing. This decision was made because these tissues were part of a larger overall study. The necessity of access to the mid-shaft and distal metaphysis for other analyses mandated by the larger study generating these bone samples made this restriction necessary. This made displacement measurements less reliable in the axial test due to axial settling of the specimen in the fixture. This is discussed further in the discussion of the axial testing results.

The analysis of the mechanical testing data includes the maximum load, the load-displacement curve, and the structural stiffness. The maximum load is reported directly by the Bluehill software and is the primary result from the

mechanical testing. The load-displacement curve was plotted using both the Bluehill software and a program, written by Scott Bouse of the Bone Biomechanics Lab, in the MATLAB software program. Stiffness was also calculated by calculating the slope of the linear region of the load-displacement curve. The linear region of the load-displacement curve was defined by visual examination and confirmed by a minimum R^2 value of 0.98.

Due to the variety and irregularities in the breaks experienced by the femoral necks during these tests, intrinsic material properties were not calculated. The lack of regular cross-sections in the breaks, in addition to the error mentioned previously in the displacement measurements, would have made intrinsic results highly inaccurate.

3.4 Estimated Strength

Strength indices provide a non-destructive method of calculating, or estimating, strength in mechanical tests of this type. Compressive strength indices and bending strength indices have both been used to estimate strength in the femoral neck region.⁽²⁶⁾ In the study done by Lang et al., the neck compressive strength index (NCSI) and neck bending strength index (NBSI) were used as estimators of strength. In that study I_x and I_y , which are used in the NBSI, are both weighted by the modulus of elasticity. In the current study NCSI and NBSI were both used and were calculated with Equations 1 and 2 listed in Section 2.6. In the current study the polar moment of inertia was used as

the combination of I_x and I_y . Further, the moment of inertia is weighted by density in the current study, as is done by the CALCBD analysis routine in the Stratec software.

A number of alternative strength indices were created in an attempt to better estimate the mechanical strength of the femoral neck, the first of these combines the NCSI and NBSI, using a formula based upon the Mohr's Circle formula which is shown in Equation 3. ⁽²⁹⁾

$$R = \sqrt{\left(\frac{\sigma_x - \sigma_y}{2}\right)^2 + \tau_{xy}^2} \quad (3)$$

In equation 3, R represents the radius of Mohr's circle. Normal stress for x and y are represented by σ_x and σ_y , respectively. Mohr's circle also takes into account any shear stresses present (τ_{xy}). The radius can be interpreted as a combined stress state when a material is subjected to multiple types of stress (bending, and axial, for example). By treating each of the indices as a stress, the indices can be combined in this fashion. Equation 4 shows the equation as it was used to combine the strength indices.

$$\text{Combined SI} = \sqrt{\left(\frac{\text{NCSI} + \text{NBSI}}{2}\right)^2} \quad (4)$$

A number of other alternative strength indices for this study were developed to further model the strength of the femoral neck. These include taking into account the vector of the load with respect to the femoral neck angle. Upon examining forty of the femoral necks included in this study, it was found the average angle

of the femoral neck relative to the shaft of the femur is 50 degrees. Figure 11 illustrates this angle and demonstrates the force components present. As shown in the figure. Both loading configurations load the femoral neck at the same relative angle. To account for this loading vector, Equations 5 and 6 were used to calculate an adjusted NCSI and NBSI. Furthermore, these were also combined using the method depicted in Equation 3 to create “combined adjusted” strength indices.

$$\text{Adjusted NCSI} = \cos(50) * \text{NCSI} \quad (5)$$

$$\text{Adjusted NBSI} = \sin(50) * \text{NBSI} \quad (6)$$

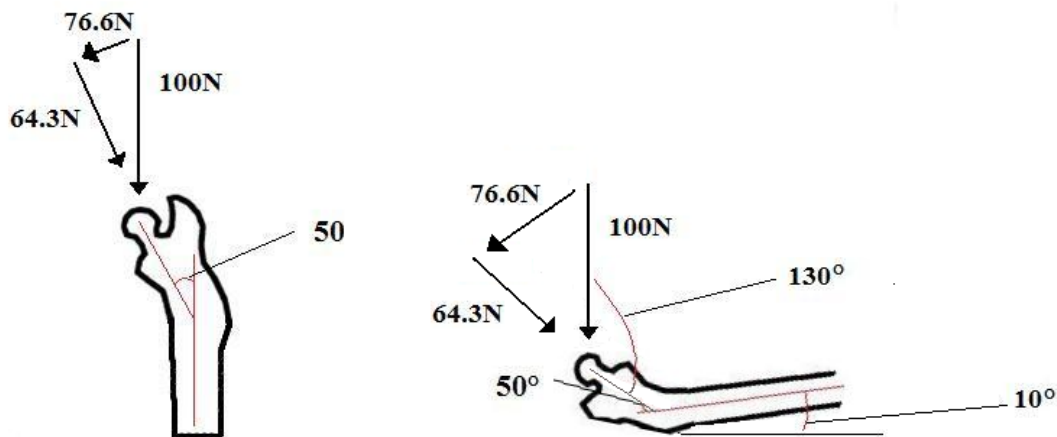


Figure 11: Loading vectors, relevant angles and example force components

3.5 Statistical Methods

Statistical significance between groups in pQCT analysis, mechanical testing and strength index calculations was determined by pair-wise comparisons derived from post-hoc testing subsequent to a two-way ANOVA

analysis which data being grouped by treatment group and time. This analysis was done as part of the Mixed Proc analysis (SAS version 9, Cary, NC). This procedure was able to handle groups of unequal sample size and data that were not normally distributed. Correlations between average mechanical maximum load values for time points and the various strength predictor averages at each time point were calculated using both linear regression models and the Pearson Correlation test (Sigmastat for Windows Ver. 3.5, Systat Software Inc.). A linear regression test quantifies a correlation with an R^2 value, the percentage of the variance. In this context, R tells the percent of the variance in mechanical strength that is determined by the strength index under study.

A Pearson Correlation test returns an R and a p value. R explains the percentage of the mechanical strength which is determined by the strength index under study. The p-value reports the statistical significance of the results. A value less than 0.05 indicates significance. Complete reports from the statistical tests for this study are in Appendix B.

4. RESULTS

During the course of the study animals were weighed once a week in order to monitor the body mass of the hindlimb unloaded (HU) animals with respect to the control animals. Figure 12 illustrates these body mass data.

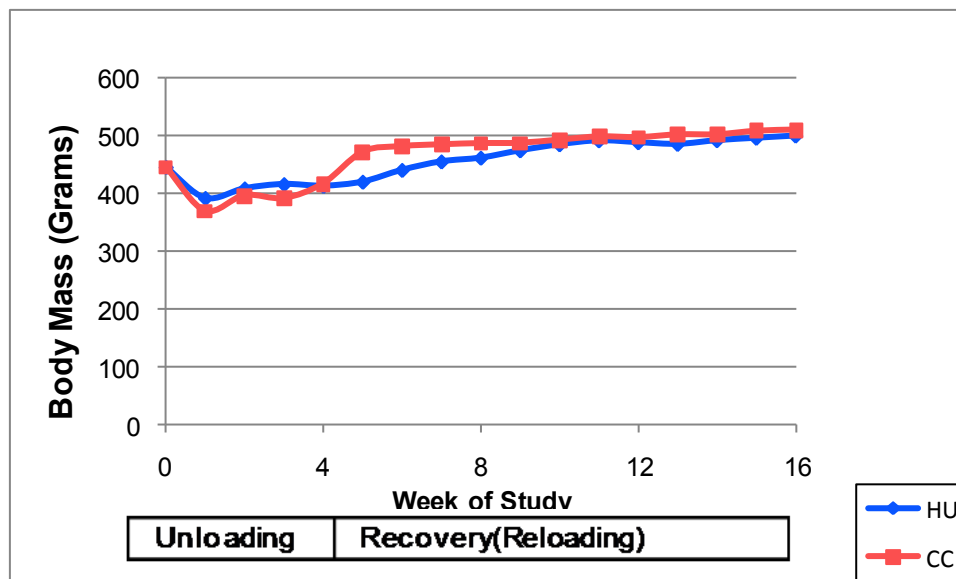


Figure 12: Weekly body mass data of combined hindlimb unloaded (HU) groups and combined cage control (CC) groups.

4.1 pQCT Data

This section presents the results of analysis of pQCT scans of the femoral neck region of the right proximal femur. Analysis was also performed on the femoral neck region of the left femur. There was no statistical difference between the results from the pQCT analysis of the right and left side. The results of the analysis on the left femora are shown in Appendix C.

The results of the analysis of pQCT scans are given in Table 1. The HU group of animals experienced a significant drop in total BMC when compared to their corresponding CC group, CC28. This difference remained at the 28 day recovery time point (REC28 vs. CC56). The HU group experienced a $6.3\% \pm 2.1\%$ (SE) drop in total BMC as compared with the baseline group that was not statistically significant.

However, there was a significant drop in cortical BMC after unloading both when comparing to baseline values and also compared to corresponding CC animals. There was also a significant rise in trabecular BMC after unloading compared to both baseline and the corresponding CC group. The increased BMC for trabecular bone, combined with a corresponding decrease in BMC for cortical bone, indicates that HU has caused resorption of bone on the endocortical surface.

The HU groups showed a significant decrease in total vBMD in both the HU and REC 28 groups compared to both baseline and the corresponding CC groups. After two recovery periods the REC56 group not only recovered to baseline values but surpassed them. vBMD values for specific compartments, cortical and trabecular, showed some significant differences from baseline. These results are also consistent with the notion that HU is causing endocortical resorption.

To better illustrate the effect of hindlimb unloading and reloading on BMC and vBMD, line graphs are included in Figures 13 and 14. These graphs display

the data for each time point as percent change from baseline values graphed versus time, where time is represented as the number of days the given group participated in the study. Similar plots are included in Appendix D for each variable in Table 1 in terms of the mean values in native units.

Table 1: Femoral Neck Bone Mineral Content (BMC) and Volumetric Bone Mineral Density (vBMD) after 28 Days of Unloading and through 84 Days of Recovery

		Day 28		Day 56		Day 84		Day 112	
	Baseline	CC28	HU	CC56	REC28	CC84	REC56	CC112	REC84
Total BMC (mg/mm)	4.87 ± 0.16	5.01 ± 0.12	4.57† ± 0.10	5.18 ± 0.12	4.75† ± 0.16	5.01 ± 0.14	4.88 ± 0.11	5.42* ± 0.15	5.25 ± 0.18
Cortical BMC (mg/mm)	4.46 ± 0.14	4.62 ± 0.10	3.87*† ± 0.10	4.72 ± 0.11	4.19† ± 0.14	4.57 ± 0.12	4.51 ± 0.10	4.96* ± 0.11	4.84* ± 0.16
Trabecular BMC (mg/mm)	0.42 ± 0.04	0.39 ± 0.05	0.70*† ± 0.04	0.46 ± 0.04	0.56* ± 0.05	0.44 ± 0.05	0.37 ± 0.03	0.46 ± 0.05	0.41 ± 0.04
Total vBMD (mg/cm ³)	1132.8 ± 15.83	1149.9 ± 13.08	1044.7*† ± 16.77	1131.0 ± 15.94	1074.5*† ± 15.60	1148.7 ± 16.88	1178.8* ± 14.77	1137.9 ± 17.21	1165.7 ± 15.94
Cortical vBMD (mg/cm ³)	1257.2 ± 12.73	1270.4 ± 11.63	1308.7*† ± 11.43	1265.1 ± 9.56	1279.3 ± 13.13	1301.0* ± 13.33	1330.5* ± 11.88	1278.6† ± 14.22	1319.8*† ± 13.77
Trabecular vBMD (mg/cm ³)	559.37 ± 7.10	555.21 ± 5.25	494.96*† ± 8.64	548.04 ± 6.70	494.33*† ± 7.10	521.97* ± 4.92	507.72* ± 7.07	522.17* ± 6.11	505.32* ± 9.3

Values are given as the group mean ± SE

* denotes that there a statistically significant difference between the mean of the group and the mean of the baseline group with a p value ≤ .05

† denotes that there a statistically significant difference between the mean of the HU group and the mean of the corresponding age-matched CC group with a p value ≤ .05

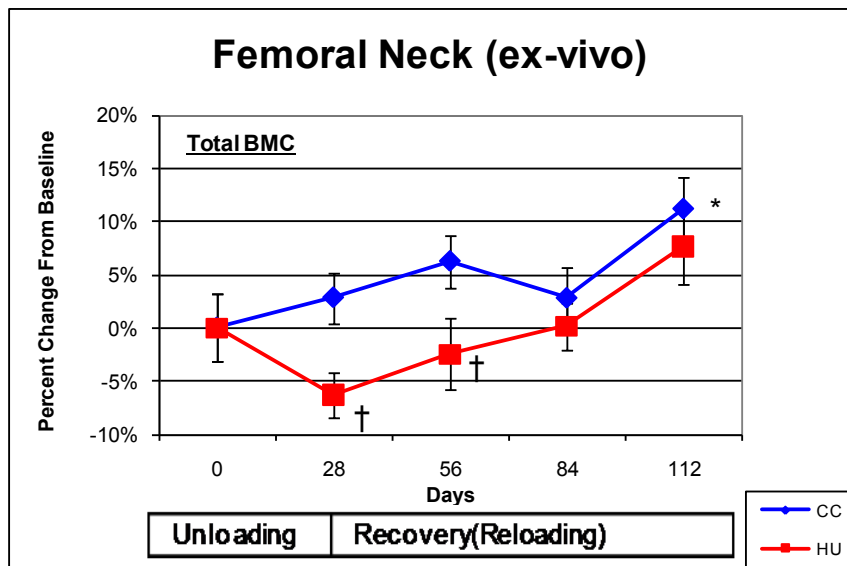


Figure 13: Percent change in total bone mineral content (BMC) in femoral neck after 28 days of hindlimb unloading (HU). CC = cage controls.

* denotes that there a statistically significant difference between the mean of the group and the mean of the baseline group with a p value $\leq .05$

† denotes that there a statistically significant difference between the mean of the HU group and the mean of the corresponding age-matched CC group with a p value $\leq .05$

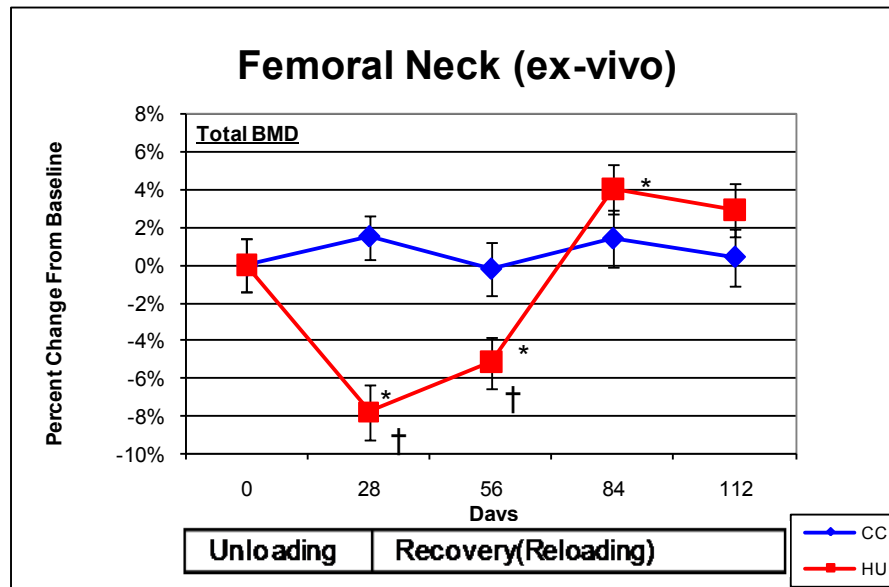


Figure 14: Percent change in total volumetric bone mineral density (vBMD) in femoral neck after 28 days of hindlimb unloading (HU). CC = cage controls.

* denotes that there a statistically significant difference between the mean of the group and the mean of the baseline group with a p value $\leq .05$

† denotes that there a statistically significant difference between the mean of the HU group and the mean of the corresponding age matched CC group with a p value $\leq .05$

Table 2 shows the results from the geometric parameters from the pQCT analysis. Unloading had no effect on Total Area. There were large changes in area in the cortical and trabecular compartments and this further confirms that the effects of HU led to cortical thinning from the endocortical surface. The fact that the Total Area remains not different from, or less than, the corresponding CC group for all time points during recovery indicates that the bone formed during reloading is being added on the endocortical surface as well. Plots similar to Figures 13 and 14 are also provided in Appendix D showing the temporal variation of the geometric pQCT parameters that are summarized in Table 2.

Table 2: Geometric Parameters from pQCT Scans of Right Femur

		Day 28		Day 56		Day 84		Day 112	
	Baseline	CC28	HU	CC56	REC28	CC84	REC56	CC112	REC84
Total Area (cm ²)	4.32 ± 0.16	4.38 ± 0.14	4.39 ± 0.12	4.61 ± 0.15	4.45 ± 0.20	4.39 ± 0.17	4.16 ± 0.13	4.80* ± 0.20	4.53 ± 0.19
Cortical Area (cm ²)	3.56 ± 0.12	3.65 ± 0.10	2.97*† ± 0.09	3.75 ± 0.11	3.30† ± 0.15	3.54 ± 0.13	3.41 ± 0.11	3.90* ± 0.13	3.69 ± 0.16
Marrow Area^A (cm ²)	0.77 ± 0.08	0.73 ± 0.08	1.42*† ± 0.10	0.86 ± 0.09	1.15*† ± 0.09	0.85 ± 0.10	0.76 ± 0.07	0.90 ± 0.11	0.84 ± 0.09
Polar Moment of Inertia (cm ⁴)	3.81 ± 0.30	3.84 ± 0.23	3.66 ± 0.20	4.12 ± 0.22	3.68 ± 0.21	3.71 ± 0.30	3.30 ± 0.15	4.53* ± 0.38	3.88 ± 0.23
Cortical Thickness (cm)	0.96 ± 0.03	1.00 ± 0.03	0.69*† ± 0.02	0.97 ± 0.03	0.81*† ± 0.03	0.94 ± 0.03	0.97 ± 0.03	0.98 ± 0.03	0.97 ± 0.04

Values are given as the group mean ± SE

* denotes that there a statistically significant difference between the mean of the group and the mean of the baseline group with a p value ≤ .05

† denotes that there a statistically significant difference between the mean of the HU group and the mean of the corresponding age-matched CC group with a p value ≤ .05

^AMarrow area is defined as area bounded by endocortical perimeter

4.2 Femoral Neck Testing Axial Loading Configuration

The right proximal femurs were tested to failure in the axial loading configuration. The properties under study in mechanical testing were maximum load and structural stiffness. As mentioned before, there was concern about error in the displacement measurements due to axial sliding, or settling, into the fixture plate. This occurs primarily at the beginning of the test as the bone slides down somewhat into the fixture. Specimens were closely monitored during testing to minimize this effect. Any specimens that were noted to move substantially and that also showed unusual deviations in their load-displacement curves were not included in the stiffness analysis. A total of 8 specimens were rejected due to these criteria. It should be emphasized as well that maximum load was not affected by such possible displacement artifacts, so data were included from all specimens for Maximum Load. The results from axial loading testing are presented in Table 3. The HU group showed a $17.1\% \pm 2.3\%$ (SE) drop in maximum load when compared to the baseline group. To better display the effect of hindlimb unloading and reloaded recovery on mechanical properties, line graphs are included in Figures 15 and 16. These graphs display the data for each time point as percent change from baseline values graphed versus time, where time is represented as the number of days the given group participated in the study.

Table 3: Axial Loading FN Test Mechanical Properties

	Day 28			Day 56		Day 84		Day 112	
	Baseline	CC28	HU	CC56	REC28	CC84	REC56	CC112	REC84
Max Load (N)	94.89 ± 4.91	97.55 ± 2.82	78.69* † ± 2.18	99.34 ± 2.16	95.53 ± 3.60	97.45 ± 3.20	102.74 ± 3.20	111.08* ± 4.93	114.85* ± 3.58
Stiffness (N/mm)	146.71 ± 7.07	143.97 ± 8.00	134.79 ± 10.08	149.77 ± 9.54	165.81 ± 8.51	169.81 ± 5.75	178.93* ± 8.26	171.37* ± 7.24	166.60 ± 8.11

Values are given as the group mean ± SE

* denotes that there a statistically significant difference between the mean of the group and the mean of the baseline group with a p value ≤ .05

† denotes that there a statistically significant difference between the mean of the HU group and the mean of the corresponding age-matched CC group with a p value ≤ .05

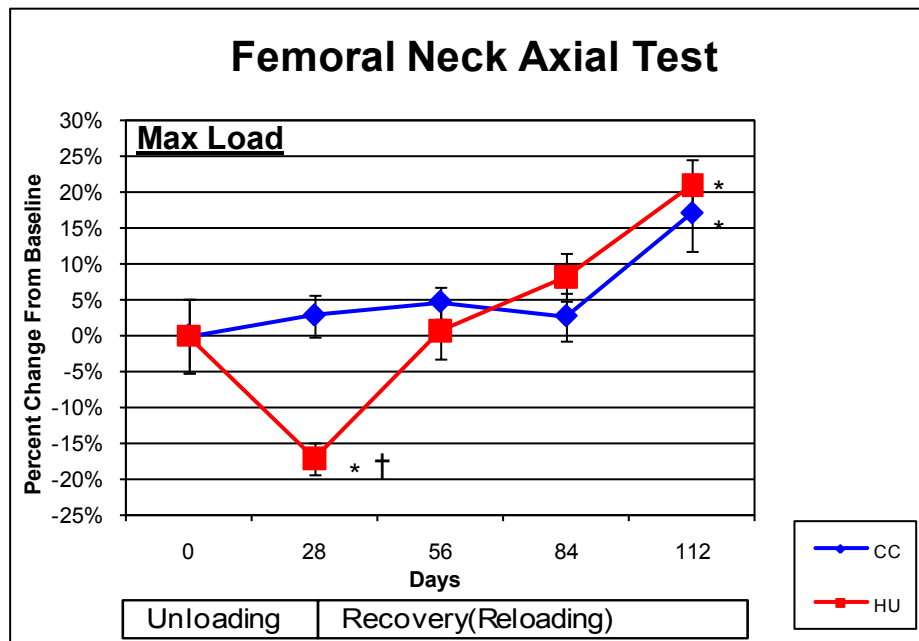


Figure 15: Maximum load sustained during FN testing for axial loading case.

* denotes that there a statistically significant difference between the mean of the group and the mean of the baseline group with a p value ≤ .05

† denotes that there a statistically significant difference between the mean of the HU group and the mean of the corresponding age-matched CC group with a p value ≤ .05

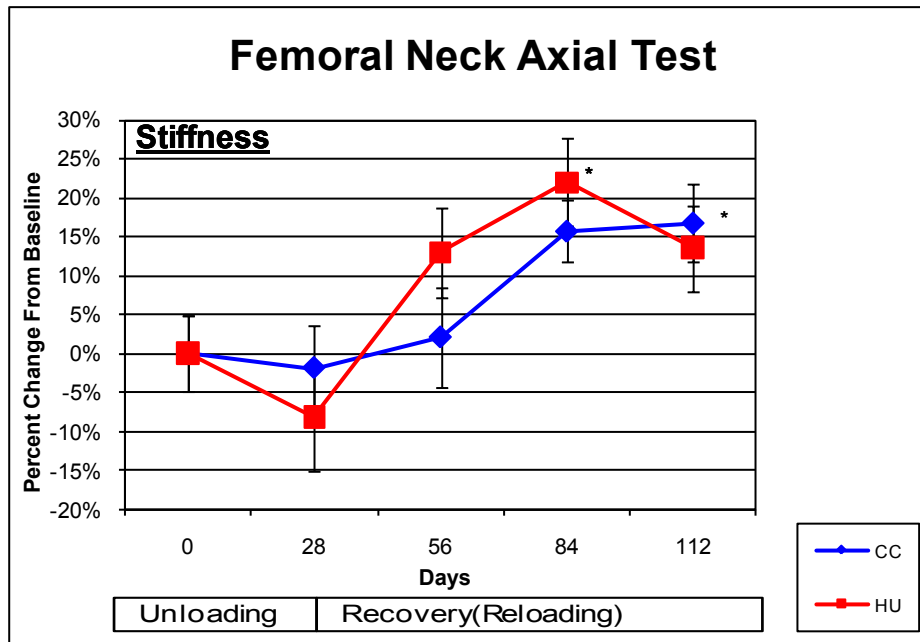


Figure 16: Stiffness of linear region during FN testing for axial loading case.
 * denotes that there a statistically significant difference between the mean of the group and the mean of the baseline group with a p value $\leq .05$
 † denotes that there a statistically significant difference between the mean of the HU group and the mean of the corresponding age-matched CC group with a p value $\leq .05$

4.3 Femoral Neck Testing Lateral Loading Configuration

The left proximal femurs were subjected to the lateral loading configuration and tested to failure. Maximum Load and Stiffness were recorded and calculated respectively, and are reported in Table 4. The HU group showed a $5.4\% \pm 1.9\%$ (SE) drop in maximum load when compared to the baseline group. This drop was not statistically significant. However the lower maximum load immediately after the 28 days of HU was significant when compared with CC animals. The maximum load recovered to within CC values in the REC56 group after two recovery periods. There was no significant treatment effect on stiffness when comparing to baseline or CC groups. However there was a non

significant drop (p value of .06) in stiffness when compared to CC groups.

Figures 17 and 18 illustrate the data for each time point as percent change from baseline values graphed versus time, where time is represented as the number of days the given group participated in the study.

Table 4: Lateral Loading FN Test Mechanical Properties

		Day 28		Day 56		Day 84		Day 112	
	Baseline	CC28	HU	CC56	REC28	CC84	REC56	CC112	REC84
Max Force (N)	88.60 ± 2.57	95.17 ± 2.40	83.79† ± 1.68	94.86 ± 2.65	85.84† ± 3.90	93.94 ± 3.97	89.20 ± 2.17	96.67 ± 2.28	102.95* ± 5.89
Stiffness (N/mm)	54.14 ± 2.71	63.49* ± 2.06	56.87 ± 1.84	63.29* ± 2.99	58.66 ± 3.08	65.45* ± 2.96	63.41* ± 3.01	64.75* ± 2.55	68.49* ± 3.88

Values are given as the group mean ± SE

* denotes that there a statistically significant difference between the mean of the group and the mean of the baseline group with a p value ≤ .05

† denotes that there a statistically significant difference between the mean of the HU group and the mean of the corresponding age-matched CC group with a p value ≤ .05

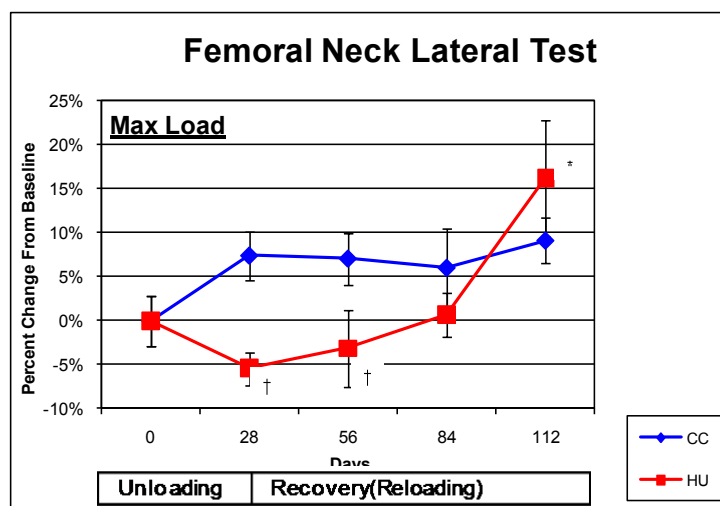


Figure 17: Maximum load sustained during FN testing for lateral loading case

* denotes that there a statistically significant difference between the mean of the group and the mean of the baseline group with a p value ≤ .05

† denotes that there a statistically significant difference between the mean of the HU group and the mean of the corresponding age-matched CC group with a p value ≤ .05

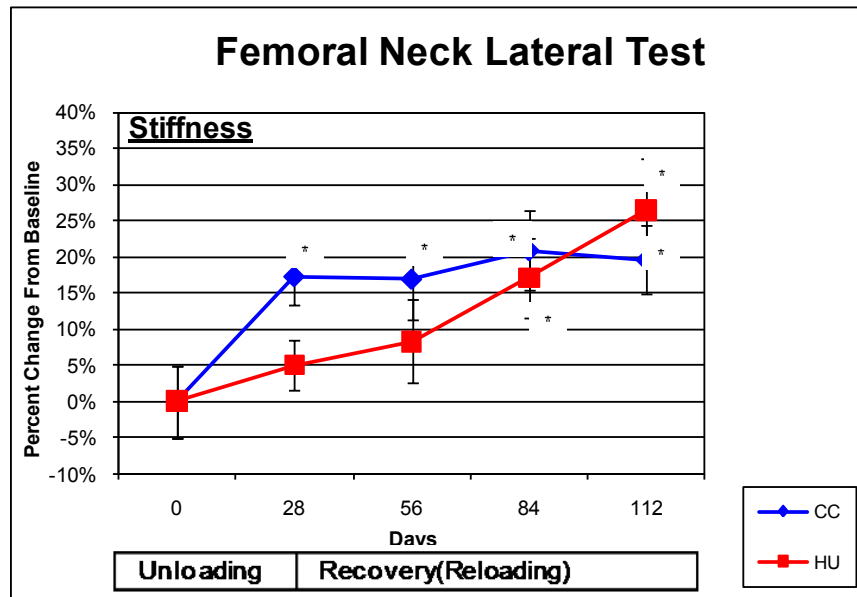


Figure 18: Stiffness of linear region during FN testing for lateral loading case.

* denotes that there a statistically significant difference between the mean of the group and the mean of the baseline group with a p value $\leq .05$

† denotes that there a statistically significant difference between the mean of the HU group and the mean of the corresponding age-matched CC group with a p value $\leq .05$

4.4 Loading Comparisons

In both the axial and lateral mechanical testing a decrease in mechanical strength was found immediately after 28 days of unloading. This decrease is shown by a drop in the maximum load sustained by the femoral neck during testing. However, the decrease did not affect the femoral neck similarly in both loading configurations. The differences in the two loading configurations can be seen in the results shown in Table 5. Figures 19 and 20 are included to better display the differences in the trends and absolute values of the HU groups in both tests.

As can be seen by the baseline averages in Table 5, the axial testing resulted in higher average loads sustained. The only exception to this is after the initial 28 days of HU. At this time point, the Maximum Load is higher for lateral loading than axial loading. In axial testing the HU group exhibited a $17.1\% \pm 2.3\%$ (SE) drop in maximum load versus baseline, whereas in lateral loading there was only a $5.4\% \pm 1.9\%$ (SE) drop. The REC28 group recovered to baseline values much faster in the axial loading configuration compared to the lateral, recovering $17.7\% \pm 3.8\%$ (SE) of the baseline average in axial loading and only $2.3\% \pm 4.4\%$ (SE) in lateral loading. This resulted in the HU groups recovering strength, evaluated as maximum load, to within baseline values in axial testing after one recovery period. The HU groups recovered lateral strength after two recovery periods.

Table 5: Comparison of Maximum Load for FN Mechanical Testing in the Two Loading

Configurations: Axial and Lateral				
	Baseline	Percent Loss at Day 28	Change in baseline percentage points between HU and REC 28	Rec Periods ^A to Return to CC
Axial	94.9 N	17.1%	17.7%	1
Lateral	88.6 N	5.4%	2.3%	2

^AOne recovery period =28 days, the duration of unloading.

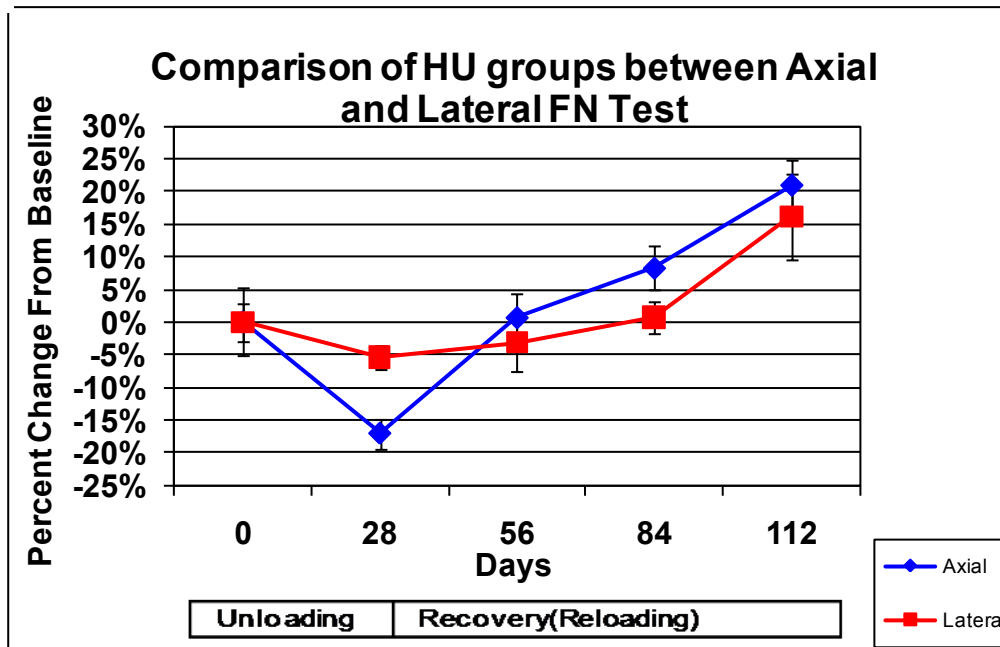


Figure 19: Loading comparisons of maximum loads sustained graphed as percent change from baseline.

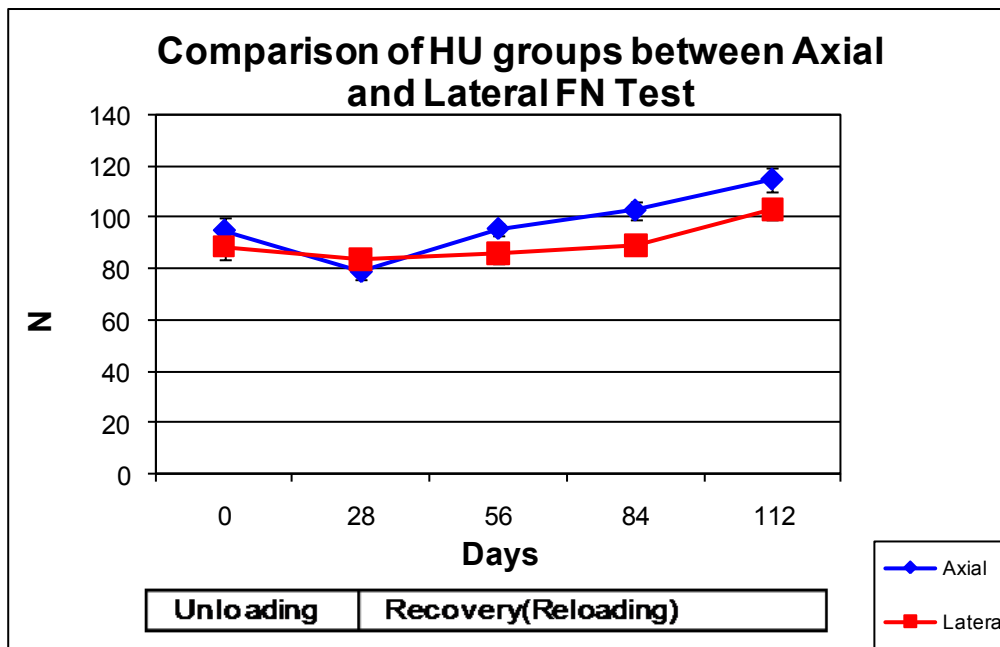


Figure 20: Loading comparisons of maximum loads sustained graphed as force vs. time point during study.

4.5 Strength Indices

Since it is not possible to perform destructive mechanical testing *in vivo* for astronauts, it is common to determine some form of calculated, or estimated, strength parameters. In this study both, estimated strengths and mechanical testing were used, highlighting one of the prominent advantages of animal models. This allowed comparison of common estimated strength indices and actual mechanical strengths. The strength indices discussed in Section 3.4, NCSI and NBSI, were used as well as the combined strength index described previously. Adjusted strength indices were also developed that incorporate the angle at which the load is applied to the axis of the femoral neck as described previously.

4.5.1 Axial Strength Indices

The strength indices discussed in Section 3.4 were calculated for each of the groups in the study. The results of these calculations are listed in Table 6. Figures 21-26 summarize results for the strength index calculation and the comparison with the tested mechanical strength, with values presented as percent change from baseline

Table 6: Axial Strength Indices

		Day 28		Day 56		Day 84		Day 112	
	Baseline	CC28	HU	CC56	REC28	CC84	REC56	CC112	REC84
NCSI (g ² /cm ⁴)	5.34 ± 0.19	5.48 ± 0.10	4.62*† ± 0.13	5.55 ± 0.09	4.78*† ± 0.11	5.39 ± 0.11	5.03 ± 0.36	5.91* ± 0.13	5.76* ± 0.16
NBSI (cm ³)	1.83 ± 0.08	1.94 ± 0.08	1.76* ± 0.05	2.01 ± 0.08	1.89 ± 0.10	1.93 ± 0.10	1.85 ± 0.07	2.11* ± 0.09	2.05* ± 0.11
Combined SI	3.58 ± 0.13	3.71 ± 0.08	3.19† ± 0.08	3.78 ± 0.07	3.33† ± 0.10	3.66 ± 0.09	3.61 ± 0.06	4.01* ± 0.10	3.90 ± 0.12
Adjusted NCSI (g ² /cm ⁴)	3.43 ± 0.12	3.52 ± 0.07	2.97*† ± 0.08	3.57 ± 0.06	3.07*† ± 0.07	3.47 ± 0.07	3.45 ± 0.06	3.80* ± 0.08	3.70* ± 0.10
Adjusted NBSI (cm ³)	1.40 ± 0.06	1.48 ± 0.06	1.35 ± 0.04	1.54 ± 0.06	1.45 ± 0.08	1.48 ± 0.08	1.42 ± 0.06	1.61* ± 0.07	1.57* ± 0.09
Combined Adj SI	2.42 ± 0.09	2.50 ± 0.06	2.16*† ± 0.05	2.56 ± 0.05	2.26† ± 0.07	2.47 ± 0.07	2.44 ± 0.04	2.71* ± 0.07	2.63* ± 0.08

Values are given as the group mean ± SE

* denotes that there a statistically significant difference between the mean of the group and the mean of the baseline group with a p value ≤ .05

† denotes that there a statistically significant difference between the mean of the HU group and the mean of the corresponding age-matched CC group with a p value ≤ .05

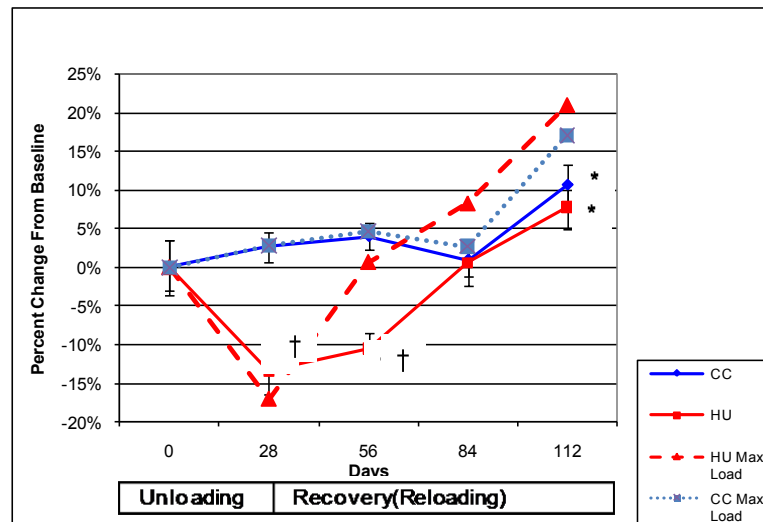


Figure 21: Neck Compression Strength Index (NCSI) calculated from right leg compared to the maximum load sustained during axial testing

* denotes that there a statistically significant difference between the mean of the group and the mean of the baseline group with a p value ≤ .05

† denotes that there a statistically significant difference between the mean of the HU group and the mean of the corresponding age-matched CC group with a p value ≤ .05

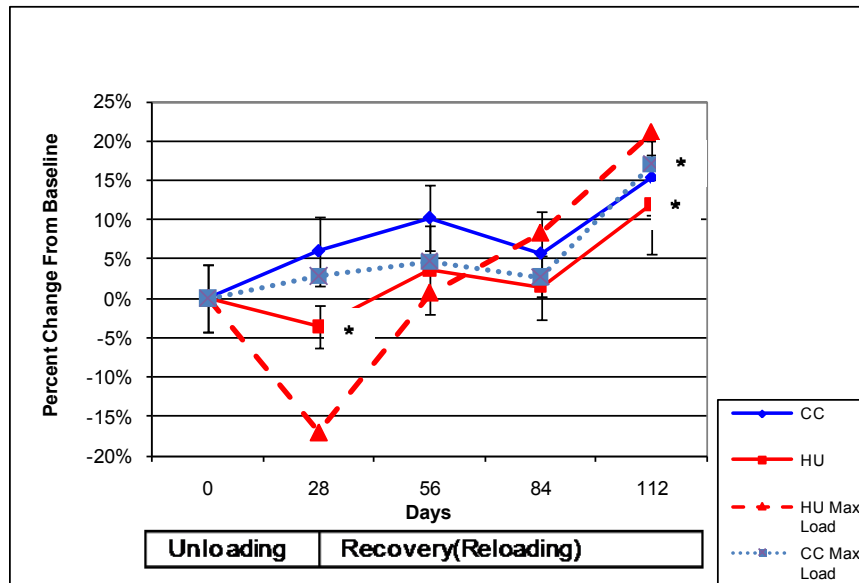


Figure 22: Neck Bending Strength Index (NBSI) calculated from right leg compared to the maximum load sustained during axial testing

* denotes that there a statistically significant difference between the mean of the group and the mean of the baseline group with a p value $\leq .05$

† denotes that there a statistically significant difference between the mean of the HU group and the mean of the corresponding age-matched CC group with a p value $\leq .05$

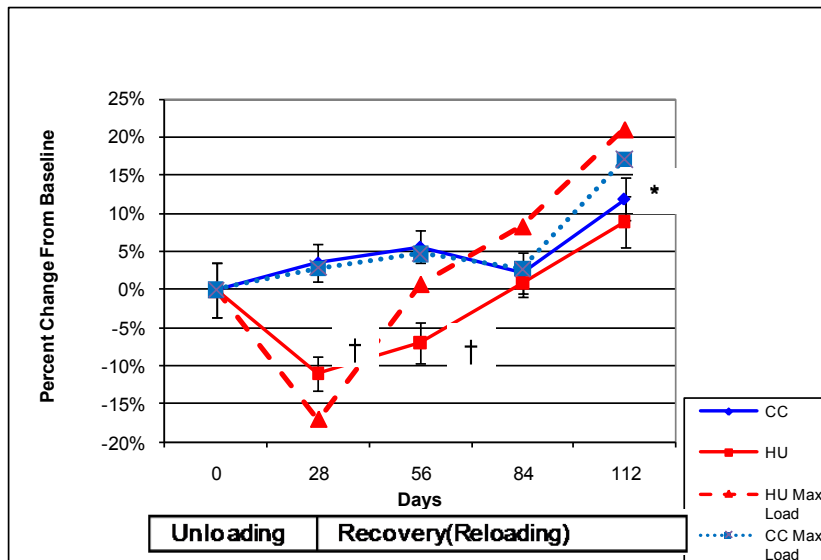


Figure 23: Combined Existing Strength Indices calculated from right leg compared to the maximum load sustained during axial testing.

* denotes that there a statistically significant difference between the mean of the group and the mean of the baseline group with a p value $\leq .05$

† denotes that there a statistically significant difference between the mean of the HU group and the mean of the corresponding age-matched CC group with a p value $\leq .05$

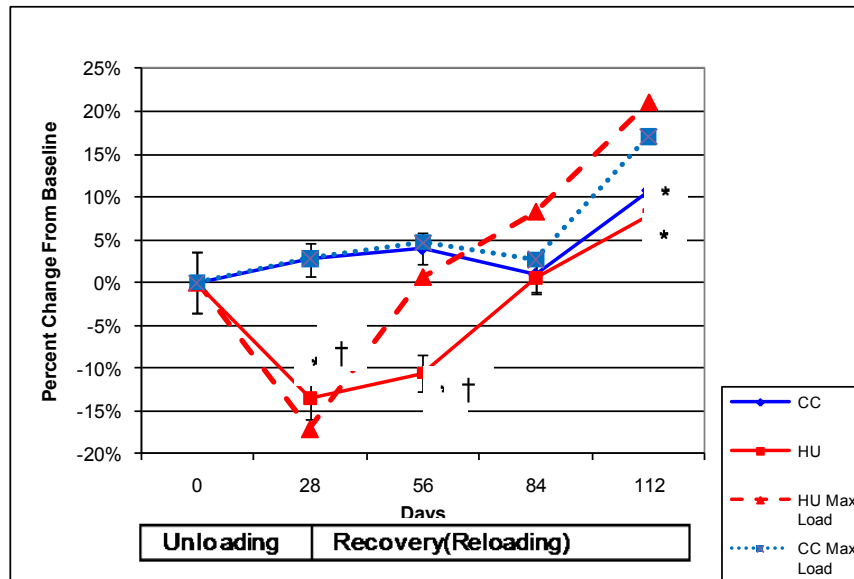


Figure 24: Adjusted Neck Compression Strength Index (adjNCSI) calculated from right leg compared to the maximum load sustained during axial testing.

* denotes that there a statistically significant difference between the mean of the group and the mean of the baseline group with a p value $\leq .05$

† denotes that there a statistically significant difference between the mean of the HU group and the mean of the corresponding age-matched CC group with a p value $\leq .05$

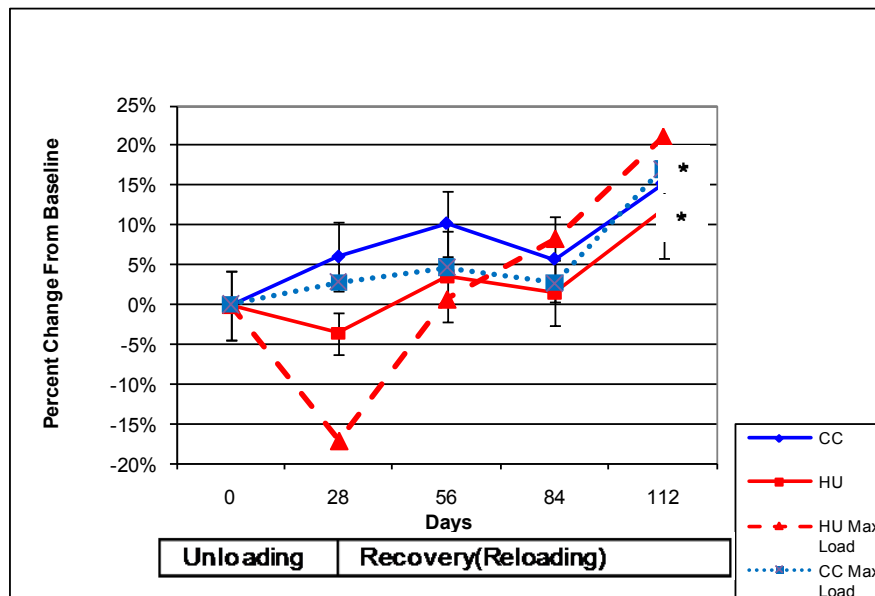


Figure 25: Adjusted Neck Bending Strength Index (adjNBSI) calculated from right leg compared to the maximum load sustained during axial testing.

* denotes that there a statistically significant difference between the mean of the group and the mean of the baseline group with a p value $\leq .05$

† denotes that there a statistically significant difference between the mean of the HU group and the mean of the corresponding age-matched CC group with a p value $\leq .05$

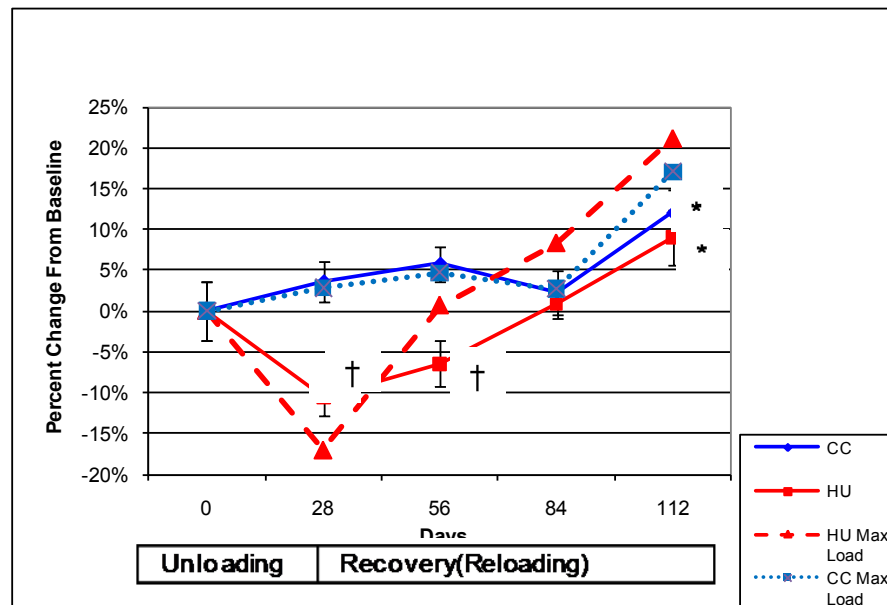


Figure 26: Combined Adjusted Strength Indices calculated from right leg compared to the maximum load sustained during axial testing.

* denotes that there a statistically significant difference between the mean of the group and the mean of the baseline group with a p value $\leq .05$

† denotes that there a statistically significant difference between the mean of the HU group and the mean of the corresponding age-matched CC group with a p value $\leq .05$

Each of the strength indices calculated were analyzed statistically to evaluate how well they predict the actual mechanical strength found from axial mechanical testing. Table 7 shows the results of three types of evaluation. The first test compared the results from each strength index plot with the mechanical testing results by linear regression using the strength index as the sole variable in a best fit regression. The adjusted R^2 value was used to quantify variance determined by the strength index under question. Using linear regression both the adjustment to existing indices and combining indices increased the correlation. However none of the strength indices correlate as well as BMC. The second test was a Pearson Correlation test to compare the correlation of each

strength index. The R value was reported to show how well the strength index correlates with the mechanical testing results and the p value gives the significance of this correlation. The same results were seen here as with linear regression, with the alternative strength indices being improvements of the existing indices and with BMC being the strongest correlation. The last assessment of the strength indices is a comparison of how well each strength index performs in predicting the magnitude of change in measured strength at day 28 immediately following the HU period. This is shown by finding the percent change from baseline for both the strength index and the mechanical testing maximum load, and then calculating the difference between the two. The strength indices (and BMC and vBMD too) all underestimated this initial reduction in strength, so the resulting values indicate the degree to which the actual reduction in strength is underestimated (in percentage points). These results are in the last column of Table 7 and show that both NCSI and the adjusted NCSI were the most accurate predictors at day 28 for the HU group.

Table 7: Strength Index Correlation for Axial Test

	Linear Regression	Pearson Correlation		% change from baseline for HU at day 28	% change from baseline for HU axial max load at day 28	difference in change scores between parameter and HU axial max load at day 28
	Adj R ²	R	p			
BMC	0.883	0.955	0.0114	6.3%	17.1%	10.8
vBMD	0.614	0.843	0.0728	7.8%	17.1%	9.3
NCSI (g²/cm⁴)	0.605	0.839	0.0757	13.4%	17.1%	3.7
NBSI (cm³)	0.766	0.908	0.033	3.6%	17.1%	13.5
Combined SI	0.781	0.935	0.0197	10.9%	17.1%	6.2
Adjusted NCSI (g²/cm⁴)	0.728	0.892	0.0419	13.4%	17.1%	3.7
Adjusted NBSI (cm³)	0.766	0.908	0.033	3.6%	17.1%	13.5
Combined Adj SI	0.846	0.94	0.0174	10.6%	17.1%	6.5

4.5.2 Lateral Strength Indices

The same strength indices calculated in the previous section were also calculated for the left femoral necks, which were tested in the lateral loading configuration. The results of these calculations are listed in Table 8. Figures 27-32 summarize results for the strength index calculations and include comparisons with the actual measured strengths from mechanical testing. All results are presented as percent change from baseline.

Table 8: Lateral Strength Indices

	Day 28			Day 56		Day 84		Day 112	
	Baseline	CC28	HU	CC56	REC28	CC84	REC56	CC112	REC84
NCSI (g ² /cm ⁴)	5.33 ± 0.15	5.53 ± 0.11	4.74*† ± 0.08	5.50 ± 0.11	4.77*† ± 0.15	5.53 ± 0.12	5.06 ± 0.36	5.71* ± 0.11	5.74* ± 0.19
NBSI (cm ³)	1.96 ± 0.07	2.04 ± 0.07	1.93 ± 0.04	2.04 ± 0.08	1.91 ± 0.07	1.94 ± 0.11	1.97 ± 0.12	2.15 ± 0.09	2.09 ± 0.08
Combined SI	3.64 ± 0.11	3.79 ± 0.08	3.33*† ± 0.06	3.77 ± 0.08	3.34*† ± 0.10	3.74 ± 0.10	3.68 ± 0.08	3.93* ± 0.08	3.92* ± 0.13
Adjusted NCSI (g ² /cm ⁴)	3.43 ± 0.10	3.55 ± 0.07	3.05*† ± 0.05	3.54 ± 0.07	3.07*† ± 0.09	3.56 ± 0.07	3.47 ± 0.06	3.67* ± 0.07	3.69* ± 0.12
Adjusted NBSI (cm ³)	1.50 ± 0.05	1.57 ± 0.05	1.48 ± 0.03	1.56 ± 0.06	1.46 ± 0.05	1.49 ± 0.08	1.51 ± 0.09	1.65 ± 0.07	1.60 ± 0.06
Combined Adj SI	2.46 ± 0.07	2.56 ± 0.06	2.26*† ± 0.04	2.55 ± 0.05	2.27*† ± 0.07	2.52 ± 0.07	2.49 ± 0.06	2.66* ± 0.05	2.65* ± 0.09

Values are given as the group mean ± SE

* denotes that there a statistically significant difference between the mean of the group and the mean of the baseline group with a p value ≤ .05

† denotes that there a statistically significant difference between the mean of the HU group and the mean of the corresponding age-matched CC group with a p value ≤ .05

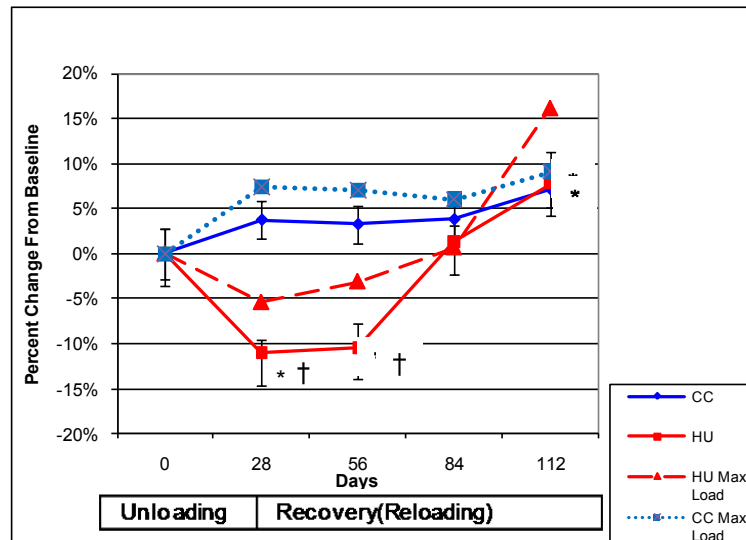


Figure 27: Neck Compressive Strength Index (NCSI) calculated from left leg compared to the maximum load sustained during lateral testing.

* denotes that there a statistically significant difference between the mean of the group and the mean of the baseline group with a p value ≤ .05

† denotes that there a statistically significant difference between the mean of the HU group and the mean of the corresponding age-matched CC group with a p value ≤ .05

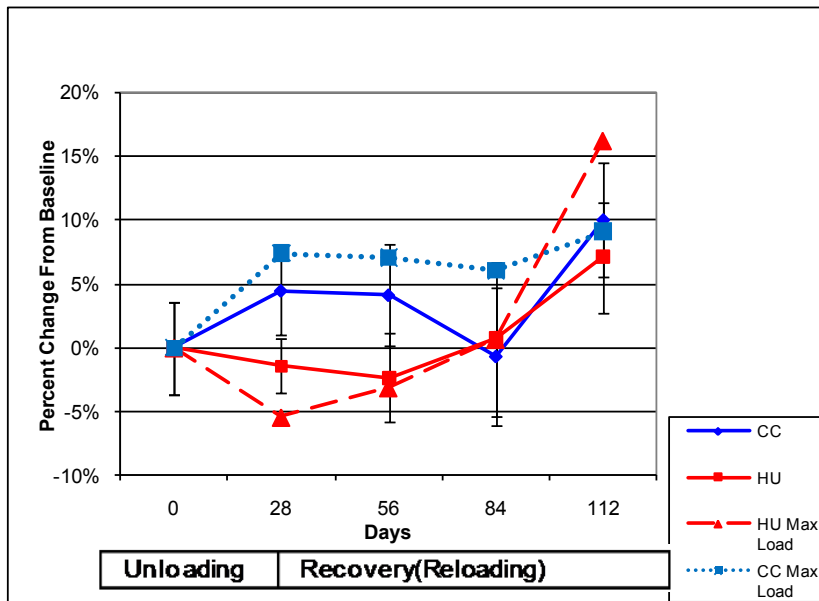


Figure 28: Neck Bending Strength Index (NBSI) calculated from left leg compared to the maximum load sustained during lateral testing.

* denotes that there a statistically significant difference between the mean of the group and the mean of the baseline group with a p value $\leq .05$

† denotes that there a statistically significant difference between the mean of the HU group and the mean of the corresponding age-matched CC group with a p value $\leq .05$

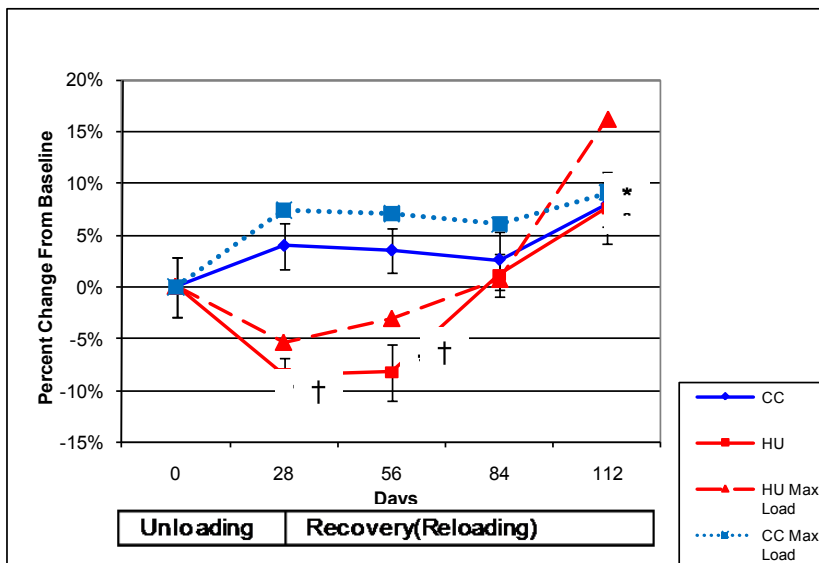


Figure 29: Combined Existing Strength Index calculated from left leg compared to the maximum load sustained during lateral testing.

* denotes that there a statistically significant difference between the mean of the group and the mean of the baseline group with a p value $\leq .05$

† denotes that there a statistically significant difference between the mean of the HU group and the mean of the corresponding age-matched CC group with a p value $\leq .05$

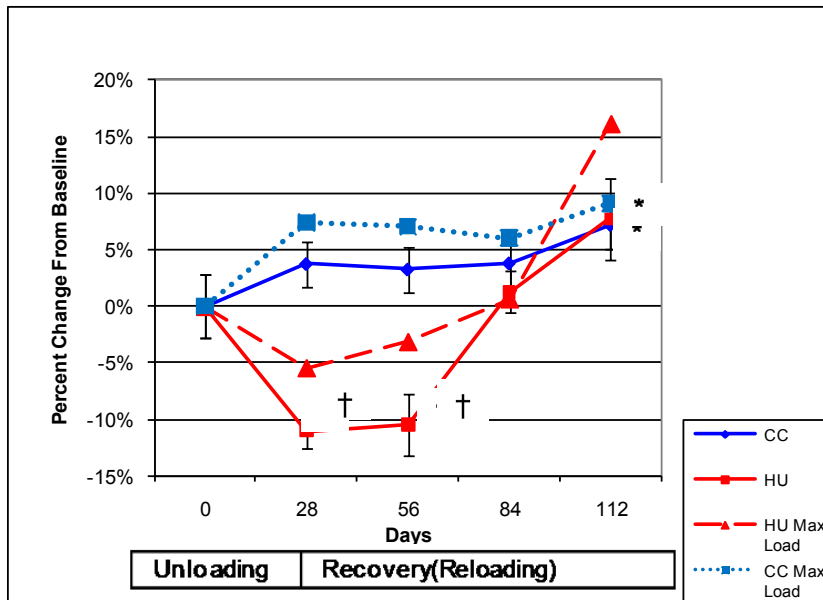


Figure 30: Adjusted Neck Compressive Strength Index (adjNCSI) calculated from left leg compared to the maximum load sustained during lateral testing.

* denotes that there a statistically significant difference between the mean of the group and the mean of the baseline group with a p value $\leq .05$

† denotes that there a statistically significant difference between the mean of the HU group and the mean of the corresponding age-matched CC group with a p value $\leq .05$

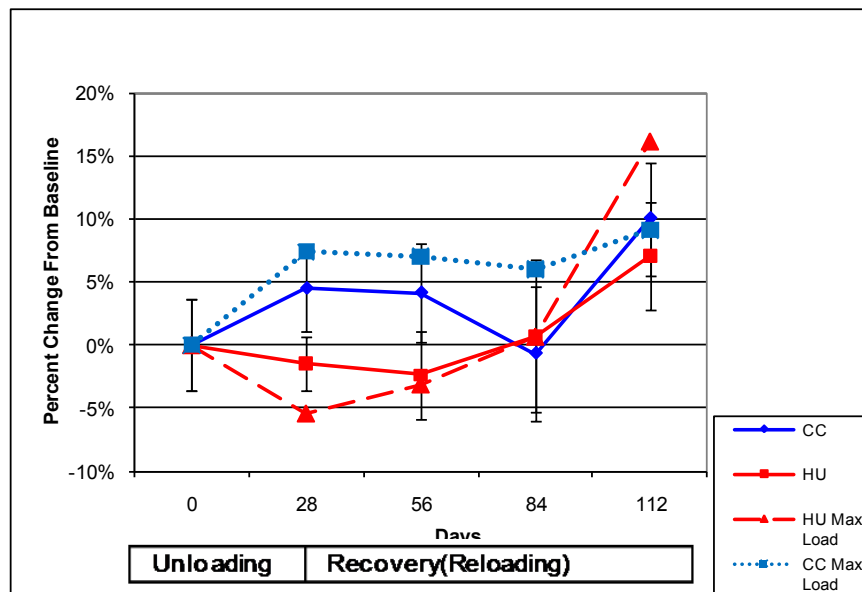


Figure 31: Adjusted Neck Bending Strength Index (adjNBSI) calculated from left leg compared to the maximum load sustained during lateral testing.

* denotes that there a statistically significant difference between the mean of the group and the mean of the baseline group with a p value $\leq .05$

† denotes that there a statistically significant difference between the mean of the HU group and the mean of the corresponding age-matched CC group with a p value $\leq .05$

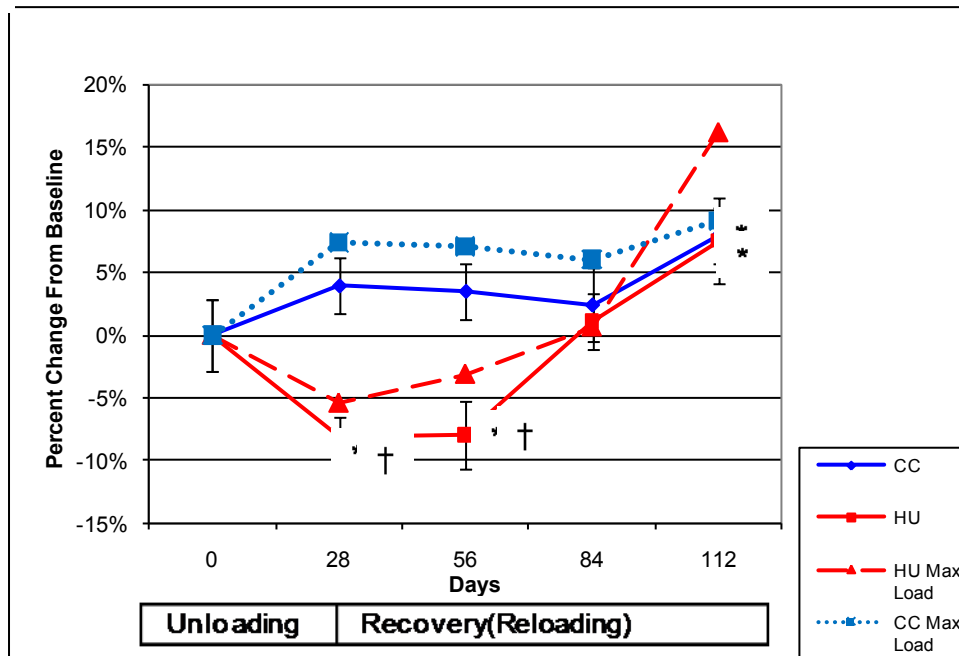


Figure 32: Combined Adjusted Strength Index calculated from left leg compared to the maximum load sustained during lateral testing.

* denotes that there a statistically significant difference between the mean of the group and the mean of the baseline group with a p value $\leq .05$

† denotes that there a statistically significant difference between the mean of the HU group and the mean of the corresponding age-matched CC group with a p value $\leq .05$

The correlations between the strength indices and the maximum load sustained during lateral testing were evaluated. Table 9 presents the results from these tests. BMC was a strong predictor for mechanical strength in the lateral loading configuration, but not as high of a correlation as seen in the axial testing. NBSI had the strongest correlation with maximum load during mechanical testing. Also no improvements were seen with the adjusted or combined strength indices. The comparison of the percent changes between the various predictors and maximum load at day 28 yielded a wide range of results(last column of Table 9). BMC was the closest with only a 1.54% difference between the two percentages. The loss in mechanical strength was

only $5.4\% \pm 1.9\%$ (SE). With such a small loss, none of the strength indices performs as a very accurate predictor at the day 28 time point.

Table 9: Strength Index Correlation for Lateral Test

	Linear Regression		Pearson Correlation		% change from baseline for HU at day 28	% change from baseline for HU lateral max load at day 28	difference in change scores between parameter and HU lateral max load at day 28
	Adj R ²	R	p				
BMC	0.801	0.922	0.0257		3.89%	5.40%	1.54
vBMD	0.209	0.638	0.247		7.23%	5.40%	1.8
NCSI (g²/cm⁴)	0.805	0.924	0.0249		11.00%	5.40%	5.57
NBSI (cm³)	0.952	0.982	0.00293		1.45%	5.40%	3.98
Combined SI	0.75	0.902	0.0365		8.46%	5.40%	3.03
Adjusted NCSI (g²/cm⁴)	0.683	0.873	0.0533		11.00%	5.40%	5.57
Adjusted NBSI (cm³)	0.952	0.982	0.00293		1.45%	5.40%	3.98
Combined Adj SI	0.761	0.906	0.0342		8.12%	5.40%	2.69

5. DISCUSSION AND SUMMARY

The overall purposes of this study were to examine the changes in bone mineralization and geometry through pQCT analysis, compare the effects of HU on measured strength from mechanical testing for different loading configurations, and evaluate the ability of strength indices to predict the mechanical strength of the femoral neck. The response of bone mineral content (BMC) and volumetric bone mineral density (vBMD) to unloading was largely congruent with previous studies. There were some interesting differences in the recovery of bone mineralization, namely with vBMD recovering more quickly than BMC.

There were differences between the effects unloading had on the mechanical strength of the femoral neck in the axial loading configuration and the lateral loading configuration. The axial configuration experienced a much greater drop in maximum load sustained during testing. However, the femoral neck recovered strength more quickly in the axial direction while the lateral direction took longer to regain strength. Again strength here is defined by the maximum load the femoral neck was able to sustain during mechanical testing to failure.

5.1 pQCT Data

The following sub-section focuses on the pQCT analysis. Two of the primary parameters of interest are BMC and vBMD. BMC allows the examination

of bone mineralization at an extrinsic or structural level, looking at the total mass in a given cross-section. vBMD on the other hand assesses the concentration of mineral in the bone tissue of the cross-section. This is looking at bone on an intrinsic or material level. The HU group experienced a $6.3\% \pm 2.1\%$ (SE) loss in total BMC after 28 days of unloading. While this loss was not a statistically significant difference from baseline, it was a significant difference from the CC control groups. After two recovery periods the REC56 group had recovered back to baseline values, and the difference between HU and cage controls at the day 84 time point (REC56 and CC84) was not statistically significant.

The loss in BMC in this thesis is smaller when compared to a previously published clinical CT study of the femoral neck in astronauts after a six month mission. ⁽²⁶⁾ The astronaut studies saw a 10.8% loss after the unloading periods (flights on the International Space Station) of durations ranging from 4 to 6 months. ⁽²⁶⁾ However the current study has a larger sample size and much greater control with respect to the length of the period subjects were unloaded. Another possible cause for the smaller drop in these rodents is the amount of trabecular bone present at the site. Rats have a much smaller ratio of trabecular to cortical bone when compared to humans as was shown in Figure 3. ⁽⁷⁾ Since trabecular bone is generally considered more metabolically active, this could account for the discrepancy.

A loss of $7.7\% \pm 1.5\%$ (SE) was seen in vBMD after the unloading period. vBMD was not recovered after one recovery period of 28 days. However, after

two recovery periods, the HU group at day 84(REC56) not only recovered to both baseline and cage control values, but surpassed baseline values by a significant difference. From this it can be inferred that vBMD recovered more quickly than BMC.

The magnitude of density loss is consistent with astronaut studies which demonstrated a 9.4% loss in BMD. ⁽²⁶⁾ However, BMD in the astronaut subjects did not recover to within baseline values after two recovery periods. ⁽²⁶⁾ A Cosmonaut study, with mission durations of 2 and 6 months, showed almost no recovery of BMD. ⁽³⁰⁾ This assessment is based on the averages for the group, and it is important to note that some individuals did experience losses. Also, the study by Vico et al. ⁽³⁰⁾ examined different anatomical sites, namely the proximal tibia and distal radius.

In HU rat studies, Bloomfield et al. showed no significant drop in vBMD in the femoral neck region, whereas the current results show a reduction due to the initial 28 days of HU of 7.8% compared to baseline and 9.1% compared to CC28. Greater agreement is observed, however, in considering other pQCT parameters. Specifically, cortical vBMD in the current study was 4.1% higher than baseline and 3.1% higher than CC28 (both statistically significant). Estimating graphically from the bar chart of the Bloomfield et al. paper ⁽¹⁰⁾, cortical vBMD at the femoral neck was approximately 4% higher than both baseline and CC (neither were statistically significant). For the cancellous compartment, trabecular vBMD was 11.5% lower due to the first 28 days of HU

compared to baseline and 10.8% lower compared to CC28. Estimating graphically again from the bar chart of the Bloomfield et al. paper⁽¹⁰⁾, they showed that trabecular vBMD was approximately 12% lower than baseline and 6% lower than CC. Once again, however the differences in the current study were statistically significant, but those of the referenced study were not.

Considering cross-sectional geometry parameters, the current study showed no significant difference in Total Area for HU compared to either baseline or CC28. The referenced study found lower mean values of Total Area (7.1% compared to baseline and 11.9% compared to CC), but the differences were not statistically significant. For the case of Cortical Area, the current results indicate reductions of 16.5% relative to baseline and 18.6% compared to CC28, and both were statistically significant. In the previous study⁽¹⁰⁾ cortical area was 10.4% lower than baseline and 14% lower than CC and both were statistically significant. IN summary the pQCT results for the first 28 days of HU for the current study match well in many respects with the previous study of Bloomfield et al.⁽¹⁰⁾ but do differ in several instances. Both studies use the same strain and gender of rats (Sprague Dawley males), and the same pQCT machine. However the current study and the Bloomfield et al. study differ on the age of the animals (6 months vs. 5 months respectively) and on the number of animals per group (15 vs. 7-10 respectively). Also, the scanner analysis settings were different. As previously described, the current study utilized a contour mode of 1, a peel mode of 1, and a threshold value of 280 mg/cm^3 , whereas the previous study

used a contour mode of 3, a peel mode of 5, and a threshold value of 214 mg/cm³.

One important consideration in pQCT scanning is the positioning of the bone sample on the CT gantry. It is notable that the CC animals showed increases in both BMC and vBMD after the first 28 days of the study. This might be considered to be the result of specimen placement inaccuracies, but this is unlikely. First, the protocols followed were very strict and adhered to carefully. Second, mechanical testing also showed increases in maximum load and stiffness for CC groups after the first 28 days, which is consistent with the pQCT results. What this also means, however, is that despite being considered to be “skeletally mature,” these Sprague Dawley rats were still experiencing some degree of skeletal growth after six months.

The endocortical resorption mentioned in Section 4.1 was clearly reflected in the densitometric and geometric results, most notably in terms of lower Cortical Area accompanied by no change in Total Area. One factor to consider related to this is whether the thresholds and other settings used in the analyses by the scanner software may have introduced errors or inaccuracies. It is in fact plausible that the trabecular bone compartment may have in fact included some amount of highly porous cortical bone tissue. Whether this should properly be considered to be trabecular bone or very porous cortical bone is problematic and not clear. It is encouraging to note that the extensive reductions in Cortical Area in the current study match quite well with the

reductions in cortical bone area in the previous study, and this is true despite the differences already noted in scan analysis parameters.

5.2 Axial Testing

Mechanical strength was directly evaluated as maximum load sustained by the femoral neck during testing. Using this evaluation, mechanical strength experienced a loss of 17.1% compared to baseline and 19.3% compared to CC28. This is a larger loss than the 9.7% loss measured in a previous HU study.⁽¹⁰⁾ comparing to baseline but quite similar to the 18.7% loss they reported compared to CC. As noted previously, the two studies are similar in many respects but also differ in other respects as well. Thus, perfect agreement would not be expected. A larger loss of 27.7% has been recorded in a leg immobilization conducted by Peng et al.⁽³¹⁾ The larger loss in mechanical strength could be explained by the fact that total immobilization removes the mobility of the lower limbs present in HU studies. Since in HU, the animals are still free to kick their legs, the leg bones are still subjected to the forces that the muscles apply. In a complete immobilization this lack of mobility more completely removes the muscle reaction forces. This could cause this treatment to have a larger effect.

The strength in the axial loading configuration recovered completely after one recovery period. This result was surprising because of the short amount of time it took for the bone to regain the strength lost during unloading. Also it was

unexpected for mechanical strength to recover before both BMC and vBMD. There was no change in the total area of the bone that could explain for this rapid recovery of strength.

It is possible that a change in the collagen content or collagen cross-linking could account for this recovery. Other studies have theorized that both collagen content and crosslinking can have an effect on bone strength.⁽³²⁾ These changes would not be apparent in the analysis that was performed as it focused on the mineralization of the bone. It is also possible that a change in the microarchitecture of the trabecular bone could be attributed to for the increase in strength. To explore this more definitively, a microCT analysis of the femoral neck could be conducted and assays done to assess composition and biochemistry.

The plate which supported the bones in the axial test allowed a certain degree of axial movement. This was due to limitations on fixation options as mentioned in Section 3.3. This may have introduced a great deal of error into the displacement measurements recorded for some cases, but the full extent of such artifacts would also depend on how well each individual sample fit into the fixture hole selected for it. Also displacement error can be introduced by flattening of the femoral head and flexure throughout the rest of the proximal femur. The axial mechanical testing did not yield any significant treatment related effects for stiffness and this may have been influenced by displacement errors or artifacts. This is difficult to know definitively, however it is possible that

with more reliable displacement measurements there might be a significant effect from unloading on stiffness. Also displacements and energy absorbed by the sample could be computed with more confidence and may very well yield valuable insight.

In order to obtain more reliable displacements, the bone specimen could be held in the same upright position as the axial testing done in this study. Instead of a single plate being used a fixture, two plates on either side of the specimen with a notch to fit the specimen could be used. These two plates could be used to clamp the bone into place in order to stop any axial motion.

5.3 Lateral Testing

The maximum load in the lateral configuration exhibited by the HU groups was not significantly lower than that of the baseline group. This is in part due to the fact that the HU group experienced a much smaller reduction in the lateral testing maximum load compared to the reductions recorded during the axial testing. Compared to the CC28 group, however, the maximum load for the HU group was lower by 12% and was statistically significant. The HU groups did not recover to within CC values until two recovery periods (56 days).

There was no significant difference between HU and CC groups in stiffness determined by the lateral femoral neck testing. Unlike the axial testing results, there was a clear trend evident in the stiffness results. There was a significant increase in stiffness from baseline values in the CC groups. This

increase was blunted by hindlimb unloading. Also there was a smaller standard error of the mean in the stiffness values for the lateral testing than the axial. This is most likely the result of greater specimen stability and less movement.

While displacement error was likely less in the lateral loading fixture, this could be improved upon. The greatest source of displacement error in the lateral loading fixture was in the rubber cushioning used under the greater trochanter. The error from the rubber cushion could be reduced either by reducing the amount of rubber used in the resting plate under the greater trochanter or by calibrating for the compressive flexing of the rubber.

5.4 Comparison of Axial and Lateral Testing (HU Effect)

As mentioned in the Section 4.4, the axial loading test demonstrated a larger decrease in maximum load for the initial 28 days of HU compared to lateral loading, namely, 17.1% as opposed to 5.4%, respectively. This is a larger difference than seen in the ovariectomy (OVX) study by Zhang et al ⁽²³⁾. Examining the effect of estrogen deficiency on bone integrity, axially loaded femoral neck specimens exhibited slightly less of a loss than laterally loaded specimens in maximum load sustained (7.0% and 8.2% respectively). ⁽²³⁾ It is somewhat expected for HU to affect bone strength in a much more direction dependent fashion than OVX. HU treatment removes an existing loading vector which stresses some regions of the femoral neck more than others. OVX causes a systemic estrogen deficiency which would affect bone quality in a more

uniform fashion. Another useful comparison is simply the difference in maximum load for axial vs. lateral loading in the two studies. In the current study at baseline, the maximum load was slightly lower for lateral loading (88.6 N vs. 94.9 N, resp.). Thus, the strength for lateral loading was 6.6% lower, but the differences were not statistically significant. In the study by Zhang et al.⁽²³⁾, strengths were compared for the two loading configurations for intact animals (i.e., not OVX), and they found the average force to be 92.8 N for axial loading and 79.8 N for lateral loading. This difference is greater than that for the current study (14.0% vs. 6.6%), and it was also statistically significant.

Additional comparisons can be made as well by considering results for other time points for the current study. As was noted in Figure 20, the maximum load was lower for lateral loading in all cases except for the HU group after the initial 28 days of unloading. In this case, the strength for lateral loading was higher (by 6.5%). For all other cases, though, the strength for lateral loading was lower, as was the case for Zhang et al.⁽²³⁾. For all of the HU plus recovery groups (REC28, REC56, REC84), the lateral loading strength was lower by 10.1%, 13.2%, and 10.4%, respectively, and these are much more consistent with the previous study (lower by 14%). Similarly, considering all of the CC groups (CC28, CC56, CC84, CC112), the strength for lateral loading was lower than for axial loading by 2.4%, 4.5%, 3.6%, and 13.0%, respectively. In comparing results for the two studies, it is also important to note some

differences. The current study used 6-month old, male, Sprague-Dawley rats, whereas the previous study used 4-month old, female, Wistar rats⁽²³⁾.

Based on human cadaver studies⁽²⁰⁾⁽²¹⁾ and the rat FN results reported by Zhang et al.⁽²³⁾, it is generally expected that the strength in lateral loading would be lower than the strength in axial loading. However, results reported by Jamsa et al.⁽²²⁾ for mice show just the opposite. The main point of their study was to study the effects of immobilization as induced in one hind leg by taping it against the abdomen. However, results are also reported for both axial and lateral loading tests for the contralateral, non-immobilized limb and also for control animals. For the contralateral limb, the strength in lateral loading was 17.2% higher than for axial loading. For control animals, the lateral strength was 7.9% higher compared to axial. In the current study, the lateral strength was 6.5% higher than the axial strength after 28 days of HU.

The HU groups recovered maximum load more quickly, when strength is determined, in the axial configuration compared to the lateral configuration. In the two configurations different surfaces were exposed to different types of stresses in each of the tests. In bending one side of the structure is in tension and the other side is in compression.

In the axial loading, the inferior surface of the femoral neck is in compression from the compressive load and the bending stress. On the superior surface, bending causes tension which works against the compressive load. In the lateral loading, the opposite is true. The superior surface is in compression

from both bending and compressive loads. It is possible that the regions of the femoral neck under the most stress in axial loading behave differently from the regions stressed under lateral loading. One possibility is that a small change in bone composition or mass will create a large change in the axial structural strength of the femoral neck. In the lateral loading configuration a larger change in bone mass or geometry is necessary to affect the femoral neck as a structure.

Another possibility is that the bone at the regions stressed in the axial loading is more sensitive to mechanical loading. This would cause the bone to exhibit a greater loss in mass and volume when unloaded and a greater anabolic effect when subjected to reloading. This would cause a faster drop, and then a faster recovery in strength. Since these changes would not be happening across the entire cross-section of the femoral neck, they would not show clearly in the pQCT results.

5.5 Strength Index Correlations

In both loading configurations, strength indices provided a higher correlation to mechanical strength than density or geometric parameters alone. This is consistent with a study that compared bending strength index with three point bending testing mechanical strength.⁽²⁷⁾ The strength index in the three point bending study followed better with mechanical strength values across a wide range of data. This is most likely due to the fact that three point bending tests create a much simpler stress state than that present in femoral neck testing.

In the axial testing comparisons, none of the strength indices had a higher correlation than total BMC. Both the NCSI and the adjusted NCSI were the most accurate at predicting the loss in strength immediately after the unloading period. While the compressive strength indices were the most predictive at the 28 day post unloading time point, they were not sufficiently predictive to replace testing. None of the strength indices were predictive at all time points.

Higher correlations between strength indices and maximum load sustained during testing were found in the lateral loading comparisons. This was mostly due to the smaller losses experienced in lateral loading strength. The 28 day comparisons were much less accurate when comparing to the magnitude of the losses experienced by the HU group.

Overall the strength indices did not make accurate predictions of mechanical strength. There were many that had moderately good correlations in both the axial and lateral testing configurations. While these could provide useful information for future studies, none of the strength indices were predictive enough at individual time points to serve as a replacement for mechanical testing. In animal studies where destructive testing is possible, strength indices would not make a suitable replacement.

It is possible that finite element analysis (FEA) might provide a more accurate predictor of bone strength. Langton et al. have shown that using FEA on a 2D radiographic image provides much more accurate prediction over BMD alone. ⁽³³⁾

5.6 Limitations

It is important to note the limitations of the HU rat model. As mentioned in Section 2.3, there are many differences between the rat femoral neck and the human femoral neck. Not only is the rat femoral neck different anatomically (relatively more cortical bone) it is also loaded differently since the rat is a quadruped while humans are bipedal. It is possible that while these SI's do not accurately predict changes in the rat femoral neck strength, they would be more accurate when applied to humans.

Another limitation to the HU model in general is the metabolism of Sprague Dawley rats. These rats continue to gain weight throughout most of their lifespan. This continual increase in body weight results in steady increases in BMC as was seen in the data from the cage control animals. This gain in BMC throughout the lifespan is not present in humans. This is the reason many of the parameters under study continue to increase in cage control animals as the study moves to later time points.

5.7 Summary

HU exposure gave rise to $6.3\% \pm 2.1\%$ (SE) lower bone mineral content (BMC) compared to BL and $7.8\% \pm 1.5\%$ (SE) lower total volumetric bone mineral density (vBMD) at the FN. These values are consistent with previous studies and demonstrate the detrimental effect that HU and disuse in general

has on bone mineralization. A unique feature of the current study is that it is the first to report on femoral neck properties and how they recover after HU.

The vertical or axial loading showed a $17.1\% \pm 2.3\%$ (SE) drop in mechanical strength due to HU exposure. The lateral loading test revealed a $5.4\% \pm 1.9\%$ (SE) drop in strength, showing that HU had a greater effect on the axial loading configuration. This demonstrates that the effect of HU is greatly influenced by the loading vectors involved. None of the strength indices completely predicted the mechanical behavior of the FN. In the right femur the combined index had the highest correlation with an R value of .94. The bending strength index had the highest correlation in the left lateral testing with an R value of .98. However the strength indices failed to predict the mechanical behavior at all the time points. None of the strength indices followed the trend of the mechanical testing results throughout the time points of the study. In general the strength indices provide valuable input but fail to replace mechanical testing.

6. FUTURE WORK

6.1 Test Fixture Refinements

As mentioned in Sections 5.2 and 5.3, the testing fixtures could be improved to give more accurate displacement measurements. The axial fixture could incorporate a clamping mechanism that would eliminate the problem of the specimen sliding axially. Reducing the thickness of the rubber cushioning in the lateral fixture under the greater trochanter would reduce compressive flexing. It would also be desirable to upgrade the apparatus that measures displacement. A linear variable differential transformer, or LVDT, could be used to limit the displacement measurements to a region more closely confined to the femoral neck. This would mean less of the flexing the shaft of the femur is experiencing would be included.

With these changes displacement and displacement-dependent structural measurements could be analyzed. Displacement, a more reliable stiffness, and the energy absorbed by the specimen would be valuable in further understanding the effects of unloading on the femoral neck.

6.2 New Strength Index Approach

This study showed that there are severe limitations to the accuracy of the strength indices evaluated. Strength indices which incorporate the bone mineral quality as well as the cross-sectional geometry are a useful starting position but do not accurately model and predict the strength of the rodent femoral neck. An

in depth structural analysis should be performed of the rodent femoral neck in an attempt to better estimate the combined stresses present in the various loading configurations. The complex loading which the femoral neck is subjected to is one of the primary reasons that current strength indices do not accurately predict mechanical behavior. These strength indices assume a single stress state.

6.3 Repeatability Studies

A group of rats with a wider range of bone mineral conditions and ages could be used to more comprehensively evaluate the repeatability of the lateral loading fixture. This also would be useful to assess the improvements for the lateral fixture suggested in the Section 6.1. This wider range of specimens could also be used to further evaluate the strength indices included in this study.

6.4 Finite Element Analysis

Finite Element Analysis, or FEA, is a very powerful computational analysis which has been used to model the human femoral neck. Using microCT a three dimensional solid model can be created. This model is broken up into finite elements which are used to estimate the stresses throughout the structure. FEA requires much more computation than strength indices, but allows intricate geometries, loading conditions and heterogeneous materials to be considered.

In order to be able to accurately model the femoral neck, microCT scans would be needed of the proximal femur. Once models are created for the

femoral neck, the main challenge is in creating an algorithm with which to estimate the elastic modulus of each element. CT scans will provide bone mineral density for each element and this data is used to estimate the elastic modulus. These algorithms are already developed for human studies. The two most promising possibilities are to either use the human algorithms for the rat models or to do experimental testing in order to develop a density modulus algorithm for rodents.

REFERENCES

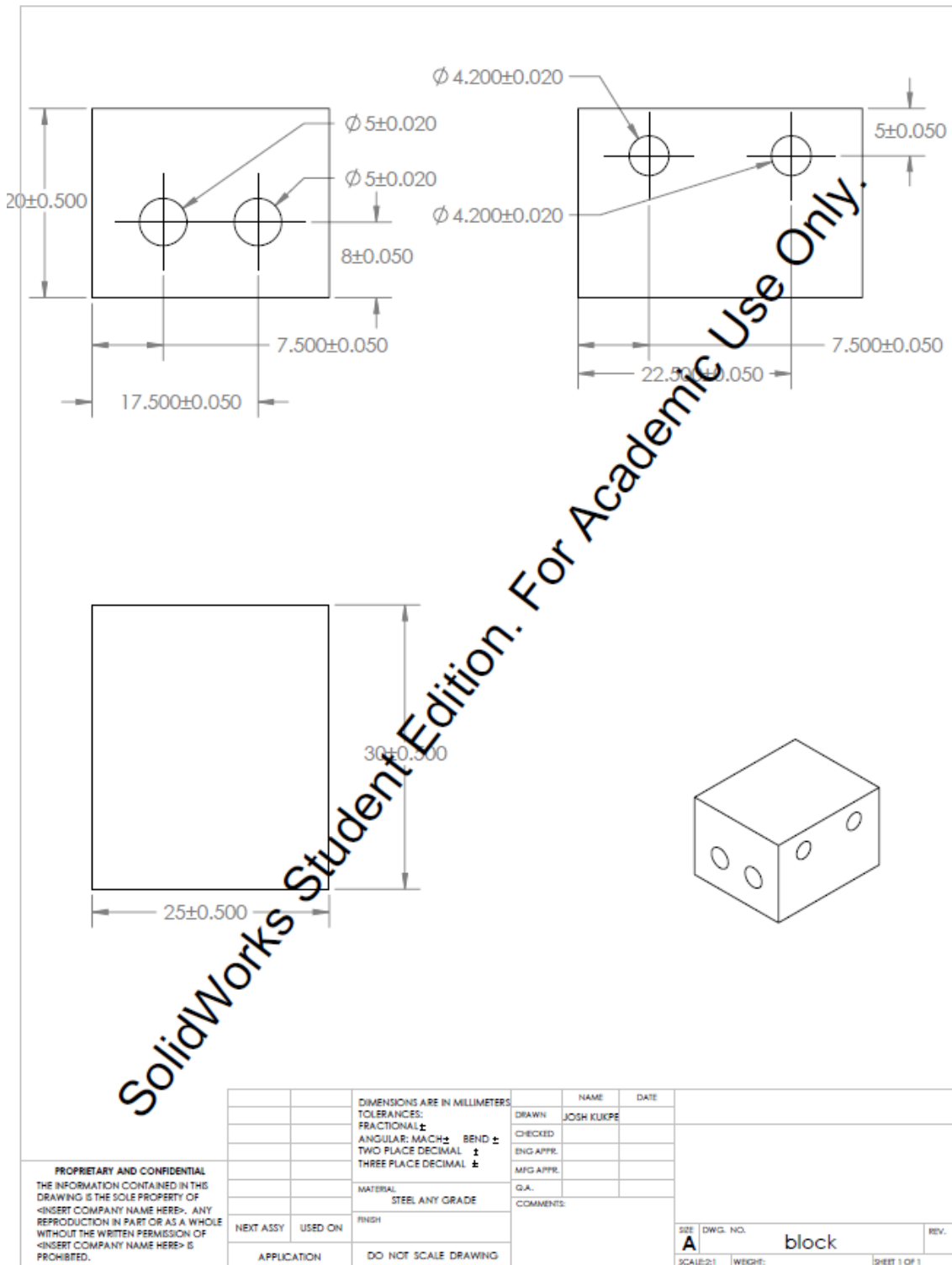
1. Turner RT. Physiology of a microgravity environment invited review: what do we know about the effects of spaceflight on bone? *J Appl Physiol.* 2000;89:840-847.
2. An YH. *Mechanical Testing of Bone and the Bone-Implant Interface.* CRC Press, Boca Raton, FL: 2000.
3. Sommerfeldt D, Rubin C. Biology of bone and how it orchestrates the form and function of the skeleton. *European Spine Journal.* 2001;S86-S95.
4. Martin RB, Burr DB, Sharkey NA. *Skeletal Tissue Mechanics.* Springer-Verlag, New York, NY: 1998.
5. Grey H. *Anatomy of the Human Body.* Lea & Febiger. Philadelphia, PA: 1918.
6. Rudman K E, Aspden R M, Meakin J R. Compression or tension? The stress distribution in the proximal femur. *Biomed Engineering Online.* 2006;5:12
7. Bagi CM, Wilkie D, Georgelos K, Williams D, Bertolini D. Morphological and structural characteristics of the proximal femur in human and rat. *Bone.* 1997;21:261-267.
8. Morey-Holton ER, Globus RK. Hindlimb unloading of growing rats: a model for predicting skeletal changes during space flight. *Bone.* 1998; 22:83S-88S.
9. Morey-Holton ER, Globus RK. 2002. Hindlimb unloading rodent model: technical aspects. *J Appl Physiol.* 2002;92:1367-1377.
10. Bloomfield SA, Allen MR, Hogan HA, Delp MD. Site- and compartment-specific changes in bone with hindlimb unloading in mature adult rats. *Bone.* 2002; 31:149-157.
11. Shimano MM, Volpon JB. Biomechanics and structural adaptations of the rat femur after hindlimb suspension and treadmill running. *Brazilian Journal of Medical and Biological Research.* 2009;42:330-338

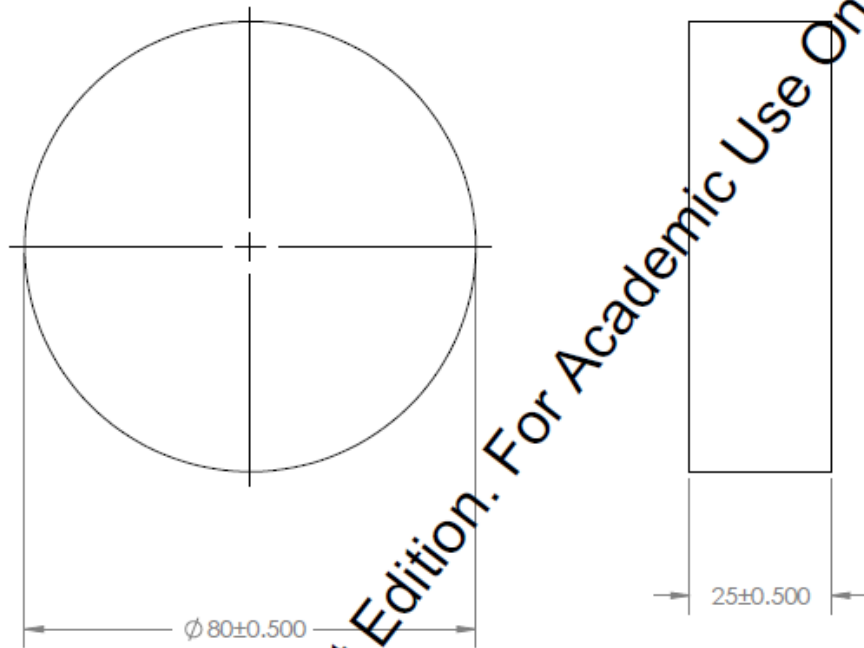
12. Kodama Y, Nakayama K, Fuse H, Fukumoto S, Kawahara H, Takahashi H, Kurokawa T, Sekiguchi C, Nakamura T, Matsumoto T. Inhibition of bone resorption by pamidronate cannot restore normal gain in cortical bone mass and strength in tail-suspended rapidly growing rats. *J Bone Miner Res.* 1997;12:1058-1067.
13. Bagi CM, Ammann P, Rizzoli R, Miller SC. Effect of estrogen deficiency on cancellous and cortical bone structure and strength of the femoral neck in rats. *Calcified Tissue International.* 1997;61: 336-344.
14. Pajamaki I, Sievanen H, Kannus P, Jokihaara J, Vuohelainen T, Jarvinen TLN. Skeletal effects of estrogen and mechanical loading are structurally distinct. *Bone.* 2008;43:748-757.
15. Jarvinen TLN, Pajamaki I, Sievanen H, Vuohelainen T, Tuukkanen J, Jarvinen M, Kannus P. Femoral neck response to exercise and subsequent deconditioning in young and adult rats. *J Bone Miner Res.* 2003;18:1292-1299.
16. Thomsen JS, Skalicky M, Viidik A. Influence of physical exercise and food restriction on the biomechanical properties of the femur of ageing male rats. *Gerontology.* 2008;54:32-39.
17. Sogaard CH, Danielsen CC, Thorling EB, Mosekilde L. Long-term exercise of young and adult femal rats: effect on femoral neck biomechanical competence and bone structure. *J Bone Miner Res.* 1994;9:409-416.
18. Prisby RD, Swift JM, Bloomfield SA, Hogan HA, Delp MD. Altered bone mass, geometry and mechanical properties during the development and progression of type 2 diabetes in the Zucker diabetic fatty rat. *J Endocrinol.* 2008;199:379-388.
19. Jämsä T, Tuukkanen J, Jalovaara P. Femoral neck strength of mouse in two loading configurations: method evaluation and fracture characteristics. *J Biomech.* 1998;31:723-729.
20. Cheng X G, Lowet G, Boonen S, Nicholson PHF, Brys P, Nijs J, Dequeker J. Assessment of the strength of proximal femur in vitro: relationship to

- femoral bone mineral density and femoral geometry. *Bone*. 1997;20:213-218.
21. Courtney AC, Wachtel EF, Myers ER, Hayes WC. Age-related reductions in the strength of the femur tested in a fall-loading configuration. *The Journal of Bone and Joint Surgery*. 1995;77:387-395
 22. Jamsa T, Koivukangas A, Ryhanen J, Jalovaara P, Tuukkanen J. Femoral neck is a sensitive indicator of bone loss in immobilized hind limb of mouse. *J Bone Miner Res*. 1999;14:1708-1713.
 23. Zhang G, Qin L, Shi Y, Leung K. A comparative study between axial compression and lateral fall configuration tested in a rat proximal femur model. *Clin Biomech*. 2005;20:729-735.
 24. Jarvinen TLN, Sievanen H, Kannus P, Jarvinen M. Dual-energy x-ray absorptiometry in predicting mechanical characteristics of rat femur. *Bone*. 1998;22:551-558.
 25. Pukkinen P, Partanen J, Jalovaara P, Jamsa T. Combination of bone mineral density and upper femur geometry improves the prediction of hip fracture. *Osteoporosis International*. 2004;15:274-280.
 26. Lang TF, Leblanc AD, Evans HJ, Lu Y. Adaptation of the proximal femur to skeletal reloading after long-duration spaceflight. *J Bone Miner Res*. 2006;21:1224-1230.
 27. Ferretti JL, Capozza RF, Zanchetta JR. Mechanical validation of a tomographic (pQCT) index for noninvasive estimation of rat femur bending strength. *Bone*. 1996;18:97-102.
 28. Jokihaara J, Jarvinen LN, Jolma P, Koobi P, Kalliovalkama J, Tuukkanen J, Saha H, Sievanen H, Kannus P, Porsti I. Renal insufficiency-induced bone loss is associated with an increase in bone size and preservation of strength in rat proximal femur. *Bone*. 2006;39:353-360.
 29. Hibbeler, RC. *Mechanics of Materials*. 5th ed. Pearson Education, Upper Saddle River, NJ: 2003.

30. Vico L, Collet P, Guignandon A, Lafage-Proust MH, Thomas T, Rehailla M, Alexandre C. Effects of long-term microgravity exposure on cancellous and cortical weight-bearing bones on cosmonauts. *The Lancet*. 2000;355:1607-1611.
31. Peng Z, Tuukkanen J, Zhang H, Jamsa T, Vaananen HK. The mechanical strength of bone in different rat models of experimental osteoporosis. *Bone*. 1994;15:523-532.
32. Bailey AJ. The role of collagen in the aging of bone. *Aging: Morphological, Biochemical, Molecular and Social Aspects*. 2002;27:217-234.
33. Langton CM, Pisharody S, Keyak JC. Comparison of 3D finite element analysis derived stiffness and BMD to determine the failure load of the excised proximal femur. *Medical Engineering and Physics*. 2009;31:668-672

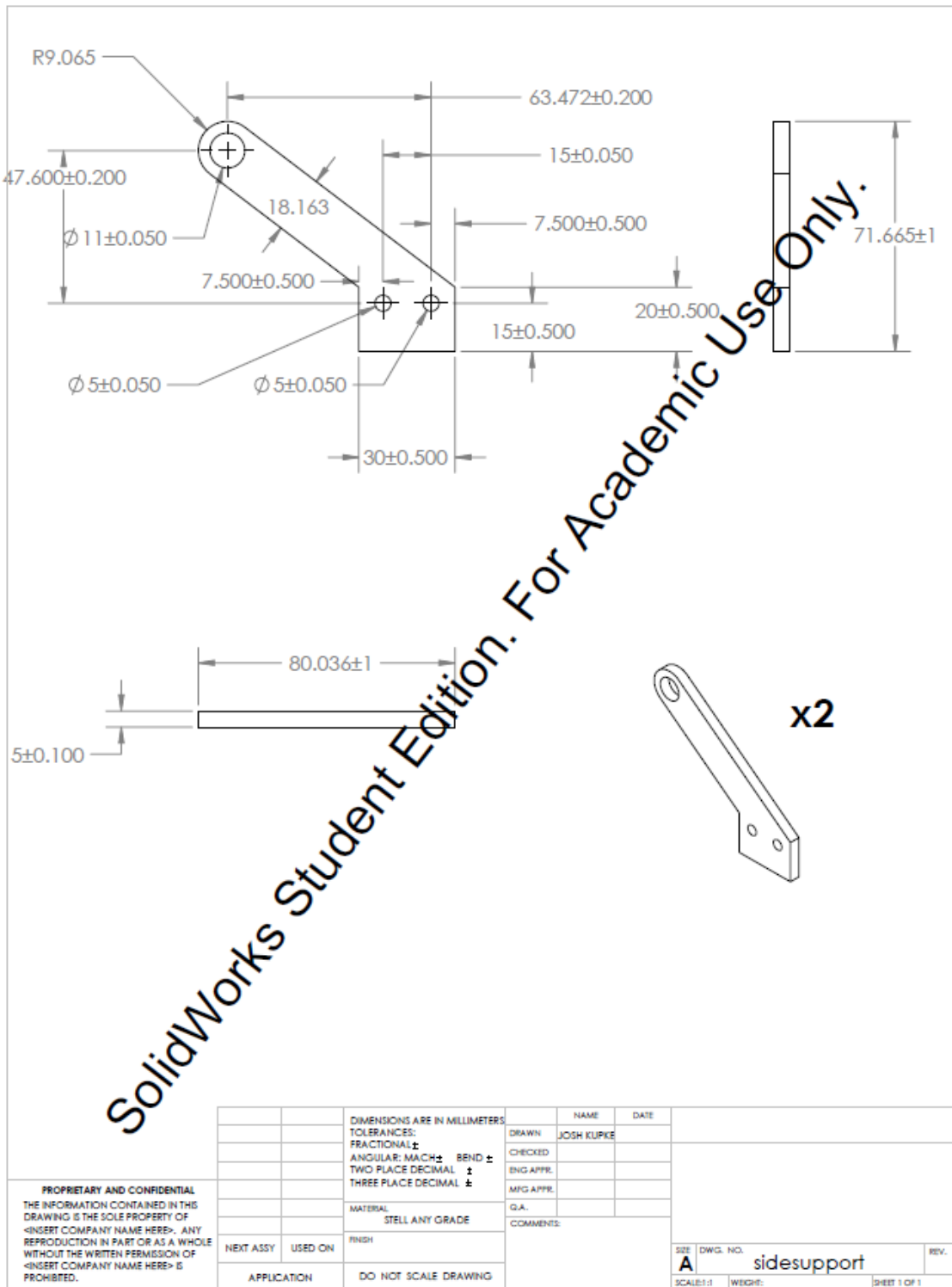
APPENDIX A
LATERAL FIXTURE ENGINEERING DRAWINGS





SolidWorks Student Edition. For Academic Use Only.

PROPRIETARY AND CONFIDENTIAL THE INFORMATION CONTAINED IN THIS DRAWING IS THE SOLE PROPERTY OF <INSERT COMPANY NAME HERE>. ANY REPRODUCTION IN PART OR AS A WHOLE WITHOUT THE WRITTEN PERMISSION OF <INSERT COMPANY NAME HERE> IS PROHIBITED.		DIMENSIONS ARE IN MILLIMETERS TOLERANCES: FRACTIONAL ± ANGULAR: MACH ± BEND ± TWO PLACE DECIMAL ± THREE PLACE DECIMAL ±		NAME JOSH KUPKE	DATE	Josh Kupke			
		MATERIAL STEEL ANY GRADE	FINISH	COMMENTS	G.A.				
NEXT ASSY	USED ON	APPLICATION	DO NOT SCALE DRAWING	SIZE A	DWG. NO. resting plate	REV.	SCALE: 1:1	WEIGHT:	SHEET 1 OF 1

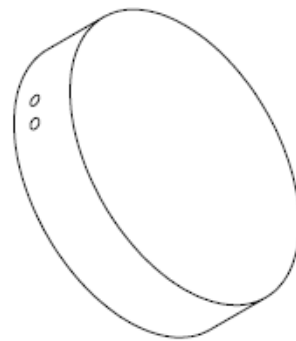
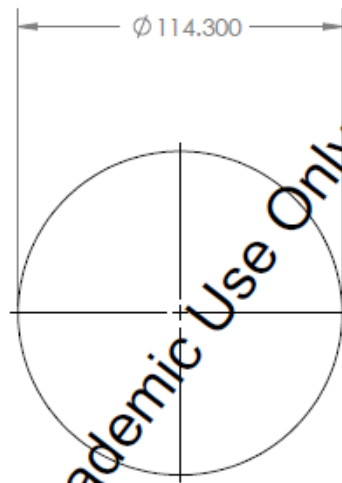
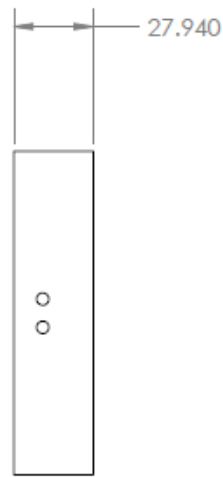


SolidWorks Student Edition. For Academic Use Only.

PROPRIETARY AND CONFIDENTIAL
 THE INFORMATION CONTAINED IN THIS
 DRAWING IS THE SOLE PROPERTY OF
 <INSERT COMPANY NAME HERE>. ANY
 REPRODUCTION IN PART OR AS A WHOLE
 WITHOUT THE WRITTEN PERMISSION OF
 <INSERT COMPANY NAME HERE> IS
 PROHIBITED.

		DIMENSIONS ARE IN MILLIMETERS		NAME	DATE
		TOLERANCES:		DRAWN	JOSH KURPKE
		FRACTIONAL: ±		CHECKED	
		ANGULAR: MACH ± BEND ±		ENG APPR.	
		TWO PLACE DECIMAL ±		MFG APPR.	
		THREE PLACE DECIMAL ±		G.A.	
		MATERIAL:		COMMENTS:	
		STELL ANY GRADE			
NEXT ASSY	USED ON	FINISH			
APPLICATION		DO NOT SCALE DRAWING			

SIZE	DWG. NO.	REV.
A	sidesupport	
SCALE: 1:1	WEIGHT:	SHEET 1 OF 1



SolidWorks Student Edition. For Academic Use Only.

<p>PROPRIETARY AND CONFIDENTIAL THE INFORMATION CONTAINED IN THIS DRAWING IS THE SOLE PROPERTY OF <INSERT COMPANY NAME HERE>. ANY REPRODUCTION IN PART OR AS A WHOLE WITHOUT THE WRITTEN PERMISSION OF <INSERT COMPANY NAME HERE> IS PROHIBITED.</p>		DIMENSIONS ARE IN MILLIMETERS		NAME	DATE
		TOLERANCES:		DRAWN	JOSH KUPKE
		FRACTIONAL: ±		CHECKED	
		ANGULAR: MACH ± BEND ±		ENG APPR.	
NEXT ASSY		USED ON		MFG APPR.	
APPLICATION		DO NOT SCALE DRAWING		G.A.	
				COMMENTS:	
				SIZE DWG. NO.	REV.
				A adjusting base	
				SCALE:1:2	WEIGHT:
				SHEET 1 OF 1	

APPENDIX B
STATISTICAL TEST REPORTS

Right Total BMC

2010 4

The SAS System

10:38 Thursday, July 8,

The Mixed Procedure

Model Information

Data Set	WORK.DATA2
Dependent Variable	TotBMC
Covariance Structure	Diagonal
Estimation Method	REML
Residual Variance Method	Profile
Fixed Effects SE Method	Model-Based
Degrees of Freedom Method	Residual

The SAS System

10:38 Thursday, July 8, 2010 5

The Mixed Procedure

Fit Statistics

AICC (smaller is better)	216.6
BIC (smaller is better)	219.4

Type 3 Tests of Fixed Effects

Effect	Num DF	Den DF	F Value	Pr > F
Group	8	123	3.67	0.0007

Least Squares Means

Effect	Group	Estimate	Standard Error	DF	t Value	Pr > t
Group	BC	4.8738	0.1355	123	35.98	<.0001
Group	CC112	5.4206	0.1402	123	38.66	<.0001
Group	CC28	5.0129	0.1355	123	37.01	<.0001
Group	CC56	5.1800	0.1355	123	38.24	<.0001
Group	CC84	5.0105	0.1402	123	35.73	<.0001
Group	HU	4.5689	0.1312	123	34.83	<.0001
Group	REC28	4.7531	0.1402	123	33.90	<.0001
Group	REC56	4.8817	0.1355	123	36.04	<.0001
Group	REC84	5.2485	0.1402	123	37.43	<.0001

Differences of Least Squares Means

Effect	Group	_Group	Estimate	Standard Error	DF	t Value	Pr > t
Group	BC	CC112	-0.5468	0.1950	123	-2.80	0.0059
Group	BC	CC28	-0.1391	0.1916	123	-0.73	0.4691
Group	BC	CC56	-0.3062	0.1916	123	-1.60	0.1125
Group	BC	CC84	-0.1367	0.1950	123	-0.70	0.4845

Group	BC	HU	0.3049	0.1886	123	1.62	0.1084
Group	BC	REC28	0.1207	0.1950	123	0.62	0.5371
Group	BC	REC56	-0.00789	0.1916	123	-0.04	0.9672
Group	BC	REC84	-0.3747	0.1950	123	-1.92	0.0570
Group	CC112	CC28	0.4077	0.1950	123	2.09	0.0386
Group	CC112	CC56	0.2406	0.1950	123	1.23	0.2195
Group	CC112	CC84	0.4101	0.1983	123	2.07	0.0407
Group	CC112	HU	0.8517	0.1920	123	4.44	<.0001
Group	CC112	REC28	0.6675	0.1983	123	3.37	0.0010
Group	CC112	REC56	0.5389	0.1950	123	2.76	0.0066
Group	CC112	REC84	0.1721	0.1983	123	0.87	0.3870
Group	CC28	CC56	-0.1671	0.1916	123	-0.87	0.3847
Group	CC28	CC84	0.002413	0.1950	123	0.01	0.9901
Group	CC28	HU	0.4440	0.1886	123	2.35	0.0201
Group	CC28	REC28	0.2598	0.1950	123	1.33	0.1852
Group	CC28	REC56	0.1312	0.1916	123	0.68	0.4947
Group	CC28	REC84	-0.2356	0.1950	123	-1.21	0.2293
Group	CC56	CC84	0.1695	0.1950	123	0.87	0.3863
Group	CC56	HU	0.6111	0.1886	123	3.24	0.0015
Group	CC56	REC28	0.4269	0.1950	123	2.19	0.0304
Group	CC56	REC56	0.2983	0.1916	123	1.56	0.1220
Group	CC56	REC84	-0.06845	0.1950	123	-0.35	0.7261
Group	CC84	HU	0.4416	0.1920	123	2.30	0.0231
Group	CC84	REC28	0.2574	0.1983	123	1.30	0.1967
Group	CC84	REC56	0.1288	0.1950	123	0.66	0.5101
Group	CC84	REC84	-0.2380	0.1983	123	-1.20	0.2324
Group	HU	REC28	-0.1842	0.1920	123	-0.96	0.3391
Group	HU	REC56	-0.3128	0.1886	123	-1.66	0.0997
Group	HU	REC84	-0.6796	0.1920	123	-3.54	0.0006
Group	REC28	REC56	-0.1286	0.1950	123	-0.66	0.5108
Group	REC28	REC84	-0.4954	0.1983	123	-2.50	0.0138
Group	REC56	REC84	-0.3668	0.1950	123	-1.88	0.0623

Right Total vBMD

2010 10

The SAS System

10:38 Thursday, July 8,

The Mixed Procedure

Model Information

Data Set	WORK.DATA5
Dependent Variable	TotBMD
Covariance Structure	Diagonal
Estimation Method	REML
Residual Variance Method	Profile
Fixed Effects SE Method	Model-Based
Degrees of Freedom Method	Residual

2010 11

The SAS System

10:38 Thursday, July 8,

The Mixed Procedure

Fit Statistics

AICC (smaller is better)	1384.9
BIC (smaller is better)	1387.6

Type 3 Tests of Fixed Effects

Effect	Num DF	Den DF	F Value	Pr > F
Group	8	123	7.65	<.0001

Least Squares Means

Effect	Group	Estimate	Standard Error	DF	t Value	Pr > t
Group	BC	1132.80	15.6437	123	72.41	<.0001
Group	CC112	1137.91	16.1927	123	70.27	<.0001
Group	CC28	1149.93	15.6437	123	73.51	<.0001
Group	CC56	1130.95	15.6437	123	72.29	<.0001
Group	CC84	1148.73	16.1927	123	70.94	<.0001
Group	HU	1044.69	15.1469	123	68.97	<.0001
Group	REC28	1074.54	16.1927	123	66.36	<.0001
Group	REC56	1178.84	15.6437	123	75.36	<.0001
Group	REC84	1165.73	16.1927	123	71.99	<.0001

Differences of Least Squares Means

Effect	Group	_Group	Estimate	Standard Error	DF	t Value	Pr > t
Group	BC	CC112	-5.1085	22.5151	123	-0.23	0.8209
Group	BC	CC28	-17.1233	22.1235	123	-0.77	0.4404
Group	BC	CC56	1.8522	22.1235	123	0.08	0.9334
Group	BC	CC84	-15.9323	22.5151	123	-0.71	0.4805

Group	BC	HU	88.1074	21.7750	123	4.05	<.0001
Group	BC	REC28	58.2641	22.5151	123	2.59	0.0108
Group	BC	REC56	-46.0344	22.1235	123	-2.08	0.0395
Group	BC	REC84	-32.9252	22.5151	123	-1.46	0.1462
Group	CC112	CC28	-12.0148	22.5151	123	-0.53	0.5946
Group	CC112	CC56	6.9607	22.5151	123	0.31	0.7577
Group	CC112	CC84	-10.8238	22.9000	123	-0.47	0.6373
Group	CC112	HU	93.2159	22.1728	123	4.20	<.0001
Group	CC112	REC28	63.3726	22.9000	123	2.77	0.0065
Group	CC112	REC56	-40.9260	22.5151	123	-1.82	0.0715
Group	CC112	REC84	-27.8167	22.9000	123	-1.21	0.2268
Group	CC28	CC56	18.9756	22.1235	123	0.86	0.3927
Group	CC28	CC84	1.1910	22.5151	123	0.05	0.9579
Group	CC28	HU	105.23	21.7750	123	4.83	<.0001
Group	CC28	REC28	75.3875	22.5151	123	3.35	0.0011
Group	CC28	REC56	-28.9111	22.1235	123	-1.31	0.1937
Group	CC28	REC84	-15.8018	22.5151	123	-0.70	0.4841
Group	CC56	CC84	-17.7845	22.5151	123	-0.79	0.4311
Group	CC56	HU	86.2552	21.7750	123	3.96	0.0001
Group	CC56	REC28	56.4119	22.5151	123	2.51	0.0135
Group	CC56	REC56	-47.8867	22.1235	123	-2.16	0.0324
Group	CC56	REC84	-34.7774	22.5151	123	-1.54	0.1250
Group	CC84	HU	104.04	22.1728	123	4.69	<.0001
Group	CC84	REC28	74.1964	22.9000	123	3.24	0.0015
Group	CC84	REC56	-30.1021	22.5151	123	-1.34	0.1837
Group	CC84	REC84	-16.9929	22.9000	123	-0.74	0.4595
Group	HU	REC28	-29.8433	22.1728	123	-1.35	0.1808
Group	HU	REC56	-134.14	21.7750	123	-6.16	<.0001
Group	HU	REC84	-121.03	22.1728	123	-5.46	<.0001
Group	REC28	REC56	-104.30	22.5151	123	-4.63	<.0001
Group	REC28	REC84	-91.1893	22.9000	123	-3.98	0.0001
Group	REC56	REC84	13.1093	22.5151	123	0.58	0.5615

Left Total BMC

The SAS System 12:32 Thursday, July 15, 2010 1

The Mixed Procedure

Model Information

Data Set	WORK.DATA1
Dependent Variable	TotBMC
Covariance Structure	Diagonal
Estimation Method	REML
Residual Variance Method	Profile
Fixed Effects SE Method	Model-Based
Degrees of Freedom Method	Residual

The Mixed Procedure

Fit Statistics

AICC (smaller is better)	202.7
BIC (smaller is better)	205.6

Type 3 Tests of Fixed Effects

Effect	Num DF	Den DF	F Value	Pr > F
Group	8	130	2.97	0.0044

Least Squares Means

Effect	Group	Estimate	Standard Error	DF	t Value	Pr > t
Group	BC	4.9838	0.1230	130	40.51	<.0001
Group	CC112	5.3374	0.1273	130	41.92	<.0001
Group	CC28	5.1936	0.1093	130	47.52	<.0001
Group	CC56	5.1524	0.1273	130	40.46	<.0001
Group	CC84	5.0604	0.1273	130	39.74	<.0001
Group	HU	4.7899	0.1065	130	44.96	<.0001
Group	REC28	4.7210	0.1273	130	37.08	<.0001
Group	REC56	5.0304	0.1230	130	40.89	<.0001
Group	REC84	5.2815	0.1273	130	41.48	<.0001

Differences of Least Squares Means

Effect	Group	_Group	Estimate	Standard Error	DF	t Value	Pr > t
Group	BC	CC112	-0.3536	0.1770	130	-2.00	0.0479
Group	BC	CC28	-0.2098	0.1646	130	-1.28	0.2046
Group	BC	CC56	-0.1686	0.1770	130	-0.95	0.3427
Group	BC	CC84	-0.07658	0.1770	130	-0.43	0.6661
Group	BC	HU	0.1939	0.1627	130	1.19	0.2357
Group	BC	REC28	0.2628	0.1770	130	1.48	0.1401
Group	BC	REC56	-0.04667	0.1740	130	-0.27	0.7889
Group	BC	REC84	-0.2978	0.1770	130	-1.68	0.0950
Group	CC112	CC28	0.1438	0.1678	130	0.86	0.3931
Group	CC112	CC56	0.1850	0.1801	130	1.03	0.3062
Group	CC112	CC84	0.2770	0.1801	130	1.54	0.1264

Group	CC112	HU	0.5475	0.1660	130	3.30	0.0013
Group	CC112	REC28	0.6164	0.1801	130	3.42	0.0008
Group	CC112	REC56	0.3069	0.1770	130	1.73	0.0854
Group	CC112	REC84	0.05583	0.1801	130	0.31	0.7570
Group	CC28	CC56	0.04122	0.1678	130	0.25	0.8064
Group	CC28	CC84	0.1332	0.1678	130	0.79	0.4286
Group	CC28	HU	0.4037	0.1526	130	2.64	0.0092
Group	CC28	REC28	0.4726	0.1678	130	2.82	0.0056
Group	CC28	REC56	0.1632	0.1646	130	0.99	0.3233
Group	CC28	REC84	-0.08795	0.1678	130	-0.52	0.6011
Group	CC56	CC84	0.09202	0.1801	130	0.51	0.6102
Group	CC56	HU	0.3625	0.1660	130	2.18	0.0308
Group	CC56	REC28	0.4314	0.1801	130	2.40	0.0180
Group	CC56	REC56	0.1219	0.1770	130	0.69	0.4922
Group	CC56	REC84	-0.1292	0.1801	130	-0.72	0.4745
Group	CC84	HU	0.2704	0.1660	130	1.63	0.1057
Group	CC84	REC28	0.3394	0.1801	130	1.88	0.0617
Group	CC84	REC56	0.02991	0.1770	130	0.17	0.8661
Group	CC84	REC84	-0.2212	0.1801	130	-1.23	0.2215
Group	HU	REC28	0.06896	0.1660	130	0.42	0.6785
Group	HU	REC56	-0.2405	0.1627	130	-1.48	0.1418
Group	HU	REC84	-0.4916	0.1660	130	-2.96	0.0036
Group	REC28	REC56	-0.3095	0.1770	130	-1.75	0.0828
Group	REC28	REC84	-0.5606	0.1801	130	-3.11	0.0023
Group	REC56	REC84	-0.2511	0.1770	130	-1.42	0.1585

Left Total vBMD

The SAS System
The Mixed Procedure

Model Information

Data Set	WORK.DATA2
Dependent Variable	TotBMD
Covariance Structure	Diagonal
Estimation Method	REML
Residual Variance Method	Profile
Fixed Effects SE Method	Model-Based
Degrees of Freedom Method	Residual

The Mixed Procedure

Fit Statistics

AICC (smaller is better)	1458.4
BIC (smaller is better)	1461.3

Type 3 Tests of Fixed Effects

Effect	Num DF	Den DF	F Value	Pr > F
Group	8	130	8.15	<.0001

Least Squares Means

Effect	Group	Estimate	Standard Error	DF	t Value	Pr > t
Group	BC	1122.99	15.3956	130	72.94	<.0001
Group	CC112	1135.03	15.9359	130	71.22	<.0001
Group	CC28	1131.07	13.6793	130	82.68	<.0001
Group	CC56	1121.87	15.9359	130	70.40	<.0001
Group	CC84	1159.13	15.9359	130	72.74	<.0001
Group	HU	1041.82	13.3329	130	78.14	<.0001
Group	REC28	1072.26	15.9359	130	67.29	<.0001
Group	REC56	1170.44	15.3956	130	76.02	<.0001
Group	REC84	1149.69	15.9359	130	72.14	<.0001

Differences of Least Squares Means

Effect	Group	_Group	Estimate	Standard Error	DF	t Value	Pr > t
Group	BC	CC112	-12.0363	22.1580	130	-0.54	0.5879
Group	BC	CC28	-8.0815	20.5948	130	-0.39	0.6954
Group	BC	CC56	1.1256	22.1580	130	0.05	0.9596
Group	BC	CC84	-36.1340	22.1580	130	-1.63	0.1054
Group	BC	HU	81.1706	20.3664	130	3.99	0.0001
Group	BC	REC28	50.7315	22.1580	130	2.29	0.0237
Group	BC	REC56	-47.4511	21.7726	130	-2.18	0.0311
Group	BC	REC84	-26.6959	22.1580	130	-1.20	0.2305
Group	CC112	CC28	3.9549	21.0018	130	0.19	0.8509
Group	CC112	CC56	13.1619	22.5368	130	0.58	0.5602
Group	CC112	CC84	-24.0976	22.5368	130	-1.07	0.2869
Group	CC112	HU	93.2069	20.7779	130	4.49	<.0001

Group	CC112	REC28	62.7679	22.5368	130	2.79	0.0062
Group	CC112	REC56	-35.4148	22.1580	130	-1.60	0.1124
Group	CC112	REC84	-14.6595	22.5368	130	-0.65	0.5165
Group	CC28	CC56	9.2070	21.0018	130	0.44	0.6618
Group	CC28	CC84	-28.0525	21.0018	130	-1.34	0.1840
Group	CC28	HU	89.2520	19.1021	130	4.67	<.0001
Group	CC28	REC28	58.8130	21.0018	130	2.80	0.0059
Group	CC28	REC56	-39.3696	20.5948	130	-1.91	0.0581
Group	CC28	REC84	-18.6144	21.0018	130	-0.89	0.3771
Group	CC56	CC84	-37.2595	22.5368	130	-1.65	0.1007
Group	CC56	HU	80.0450	20.7779	130	3.85	0.0002
Group	CC56	REC28	49.6060	22.5368	130	2.20	0.0295
Group	CC56	REC56	-48.5767	22.1580	130	-2.19	0.0301
Group	CC56	REC84	-27.8214	22.5368	130	-1.23	0.2192
Group	CC84	HU	117.30	20.7779	130	5.65	<.0001
Group	CC84	REC28	86.8655	22.5368	130	3.85	0.0002
Group	CC84	REC56	-11.3171	22.1580	130	-0.51	0.6104
Group	CC84	REC84	9.4381	22.5368	130	0.42	0.6761
Group	HU	REC28	-30.4390	20.7779	130	-1.46	0.1453
Group	HU	REC56	-128.62	20.3664	130	-6.32	<.0001
Group	HU	REC84	-107.87	20.7779	130	-5.19	<.0001
Group	REC28	REC56	-98.1826	22.1580	130	-4.43	<.0001
Group	REC28	REC84	-77.4274	22.5368	130	-3.44	0.0008
Group	REC56	REC84	20.7552	22.1580	130	0.94	0.3507

Left Right Comparison

Total BMC

The Mixed Procedure

Fit Statistics

-2 Res Log Likelihood	416.4
AIC (smaller is better)	418.4
AICC (smaller is better)	418.4
BIC (smaller is better)	422.0

Type 3 Tests of Fixed Effects

Effect	Num DF	Den DF	F Value	Pr > F
Group	8	253	6.43	<.0001
leg	1	253	1.19	0.2759
Group*leg	8	253	0.34	0.9496

Total VBMD

The Mixed Procedure

Fit Statistics

-2 Res Log Likelihood	2839.2
AIC (smaller is better)	2841.2
AICC (smaller is better)	2841.3
BIC (smaller is better)	2844.8

Type 3 Tests of Fixed Effects

Effect	Num DF	Den DF	F Value	Pr > F
Group	8	253	15.62	<.0001
leg	1	253	0.82	0.3660
Group*leg	8	253	0.15	0.9963

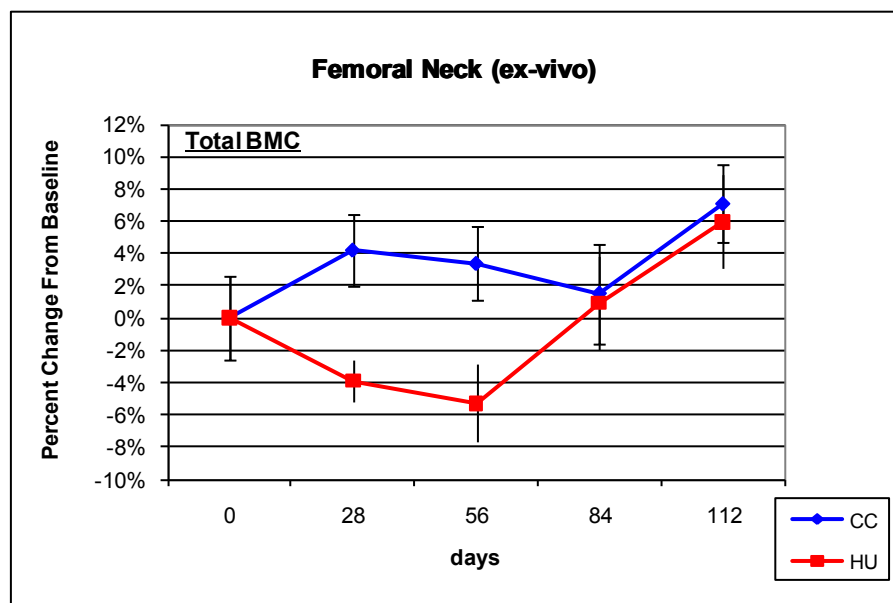
APPENDIX C
LEFT FEMUR PQCT ANALYSIS

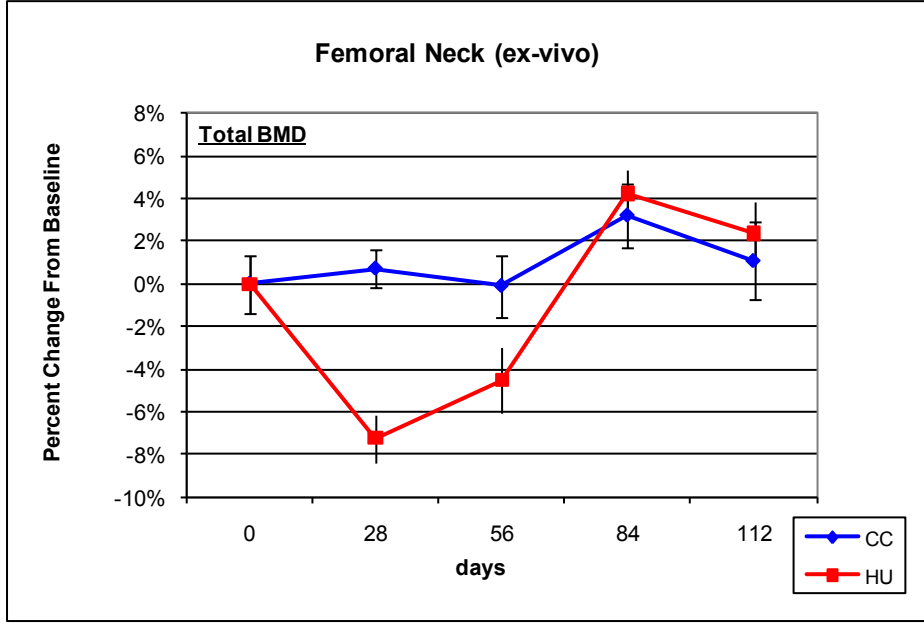
	Baseline	CC28	HU	CC56	REC28	CC84	REC56	CC112	REC84
Total BMC (mg/mm)	4.98 ± 0.13	5.19 ± 0.11	4.79† ± 0.07	5.15 ± 0.11	4.72† ± 0.12	5.06 ± 0.15	5.03 ± 0.15	5.34* ± 0.12	5.28* ± 0.15
Cortical BMC (mg/mm)	4.47 ± 0.12	4.68 ± 0.10	4.08*† ± 0.06	4.59 ± 0.09	4.11*† ± 0.11	4.61 ± 0.12	4.62 ± 0.14	4.84* ± 0.09	4.79* ± 0.14
Trabecular BMC (mg/mm)	0.52 ± 0.04	0.51 ± 0.03	0.71*† ± 0.03	0.56 ± 0.04	0.61 ± 0.04	0.45 ± 0.04	0.41* ± 0.02	0.50 ± 0.06	0.49 ± 0.05
Total VBMD (mg/cm ³)	1122.99 ± 15.25	1131.07 ± 9.97	1041.82*† ± 12.64	1121.87 ± 16.43	1072.26*† ± 17.15	1159.13 ± 17.04	1170.4 4* ± 12.8	1135.0 3 ± 20.5	1149.6 9 ± 16.95
Cortical BMD (mg/cm ³)	1286.31 ± 8.53	1292.45 ± 10.51	1324.28*† ± 8.42	1315.40 ± 9.48	1325.34* ± 5.85	1332.18 * ± 8.97	1335.8* ± 13.22	1309.7 9 ± 16.1	1352.2 9*† ± 11.38
Trabecular BMD (mg/cm ³)	538.25 ± 6.01	533.68 ± 5.16	467.18*† ± 7.79	515.46 ± 11	473.56*† ± 11.18	503.84* ± 11.61	497.45* ± 6.89	496.68 * ± 10.5	475.96* ± 10.85

Values are given as the group mean ± SEM

* denotes that there a statistically significant difference between the mean of the group and the mean of the baseline group with a p value ≤ .05

† denotes that there a statistically significant difference between the mean of the HU group and the mean of the corresponding age-matched CC group with a p value ≤ .05

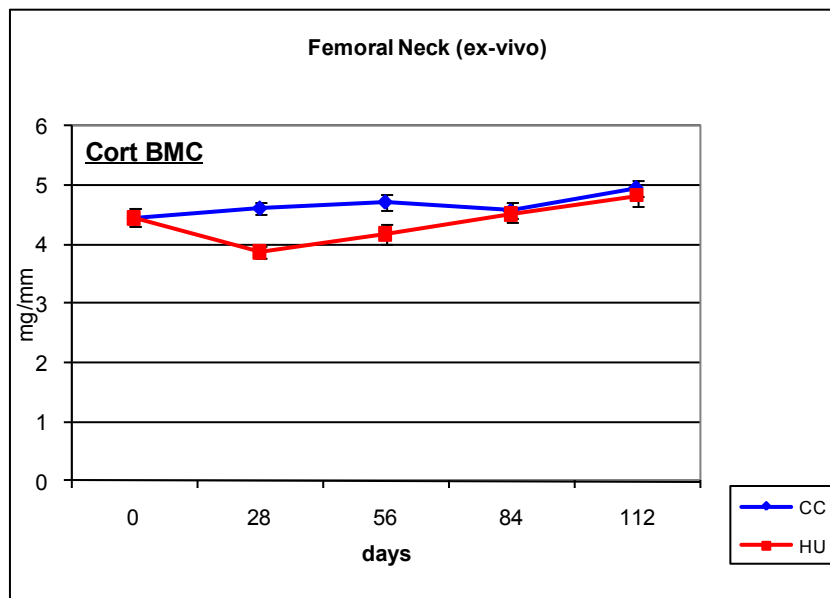
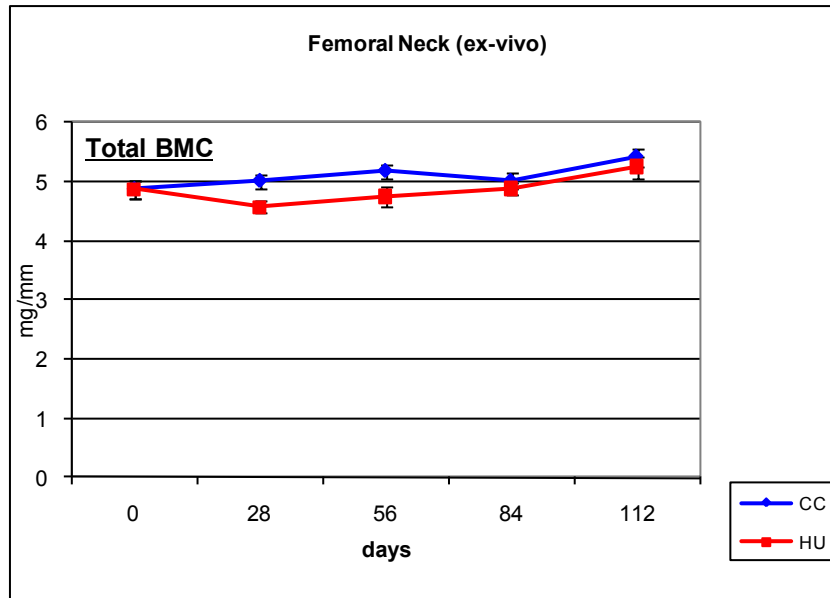


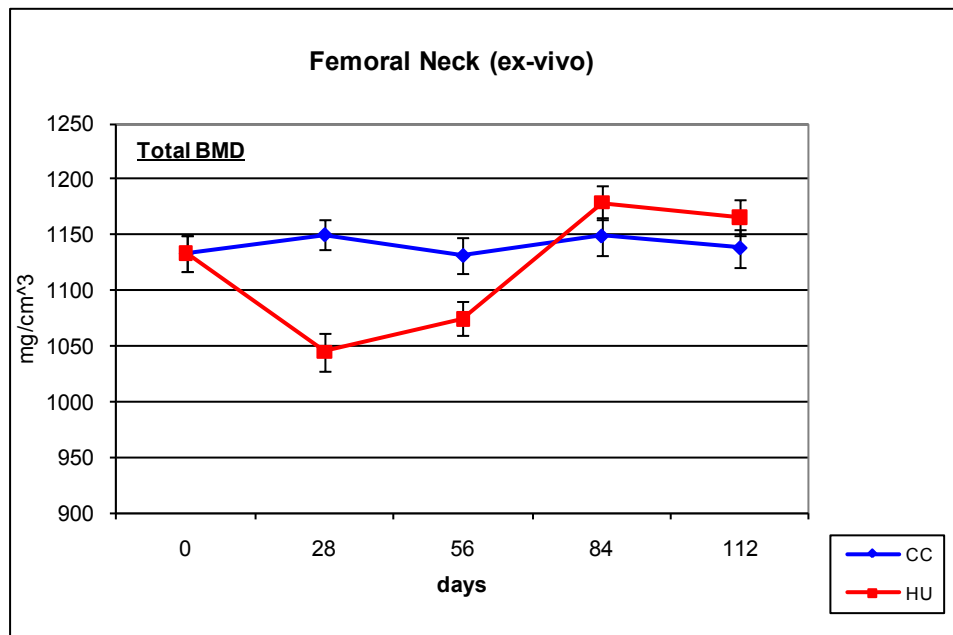
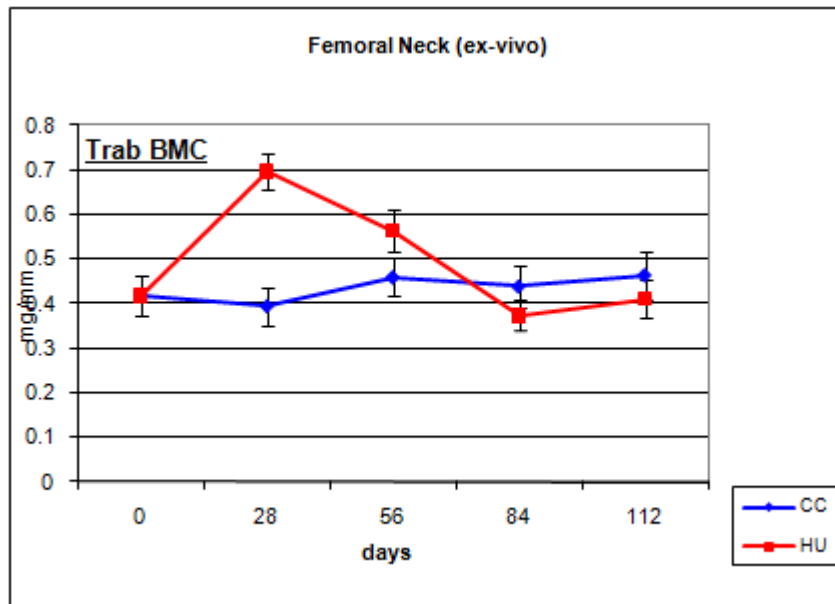


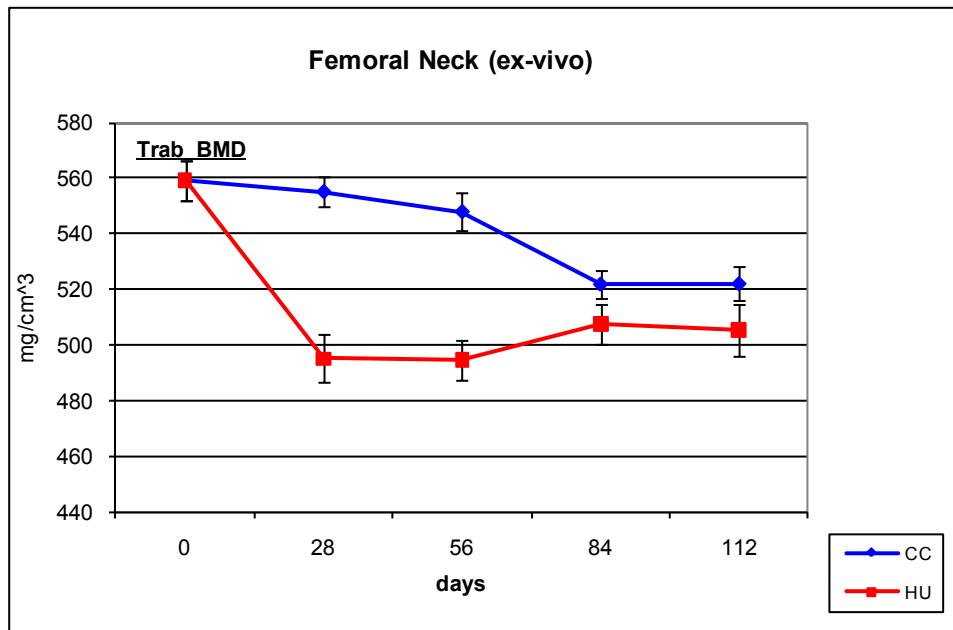
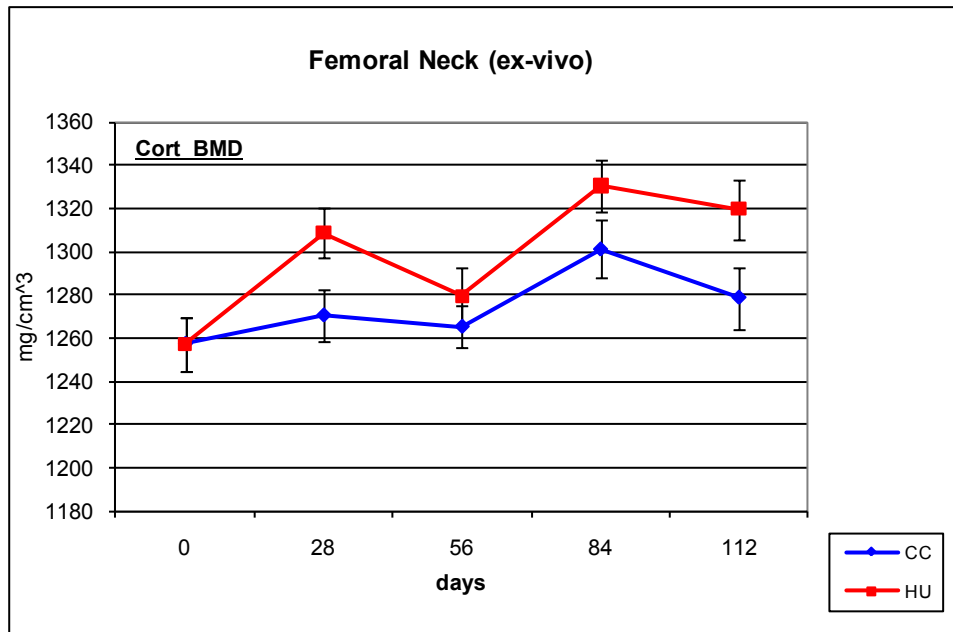
APPENDIX D

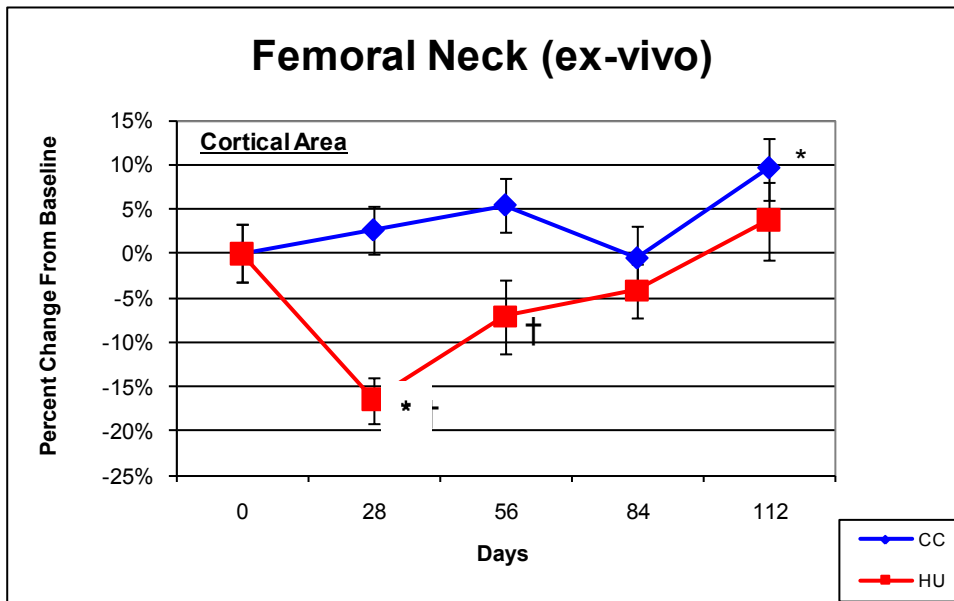
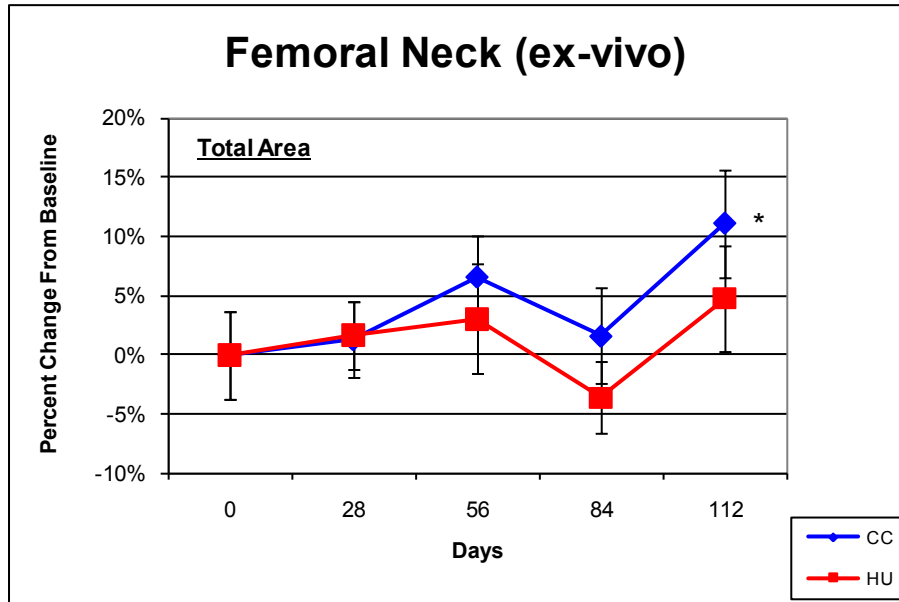
RIGHT PQCT ABSOLUTE VALUE GRAPHS AND

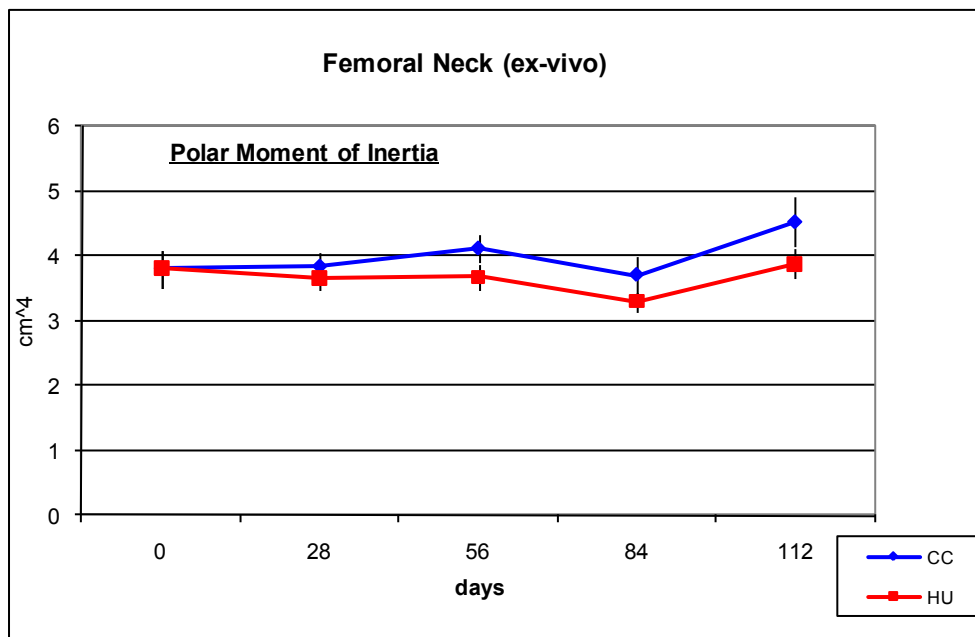
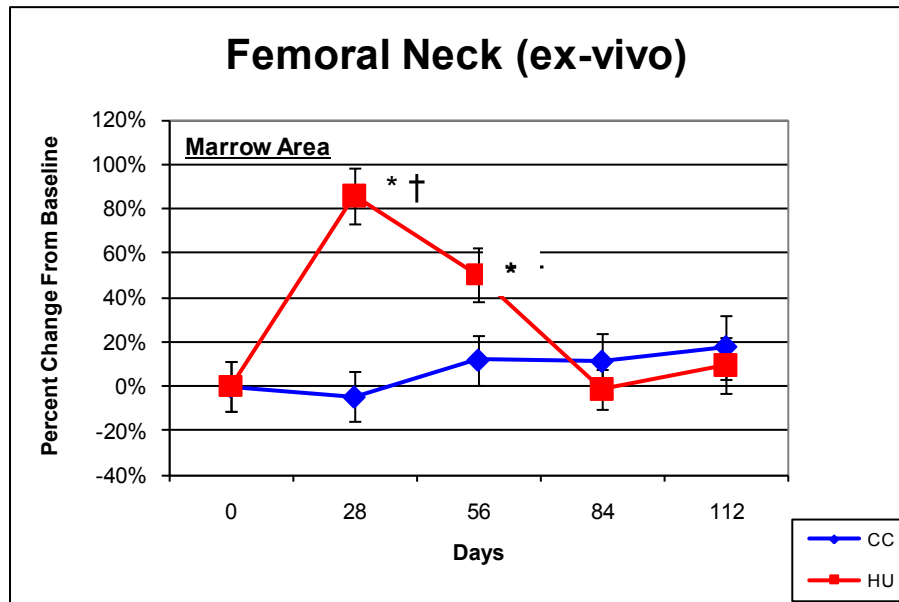
RIGHT PQCT GEOMETRIC PARAMETER GRAPHS

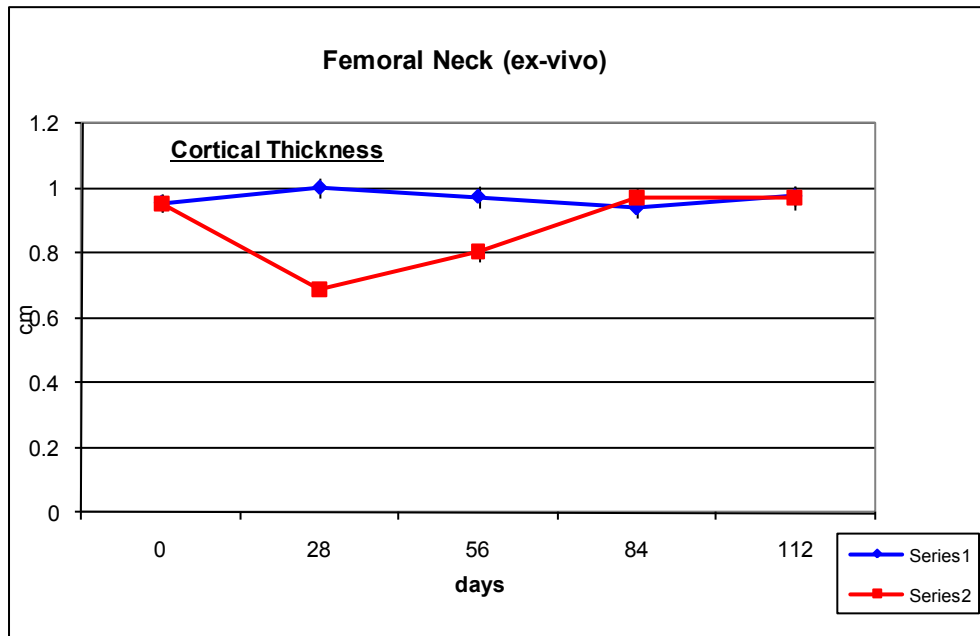






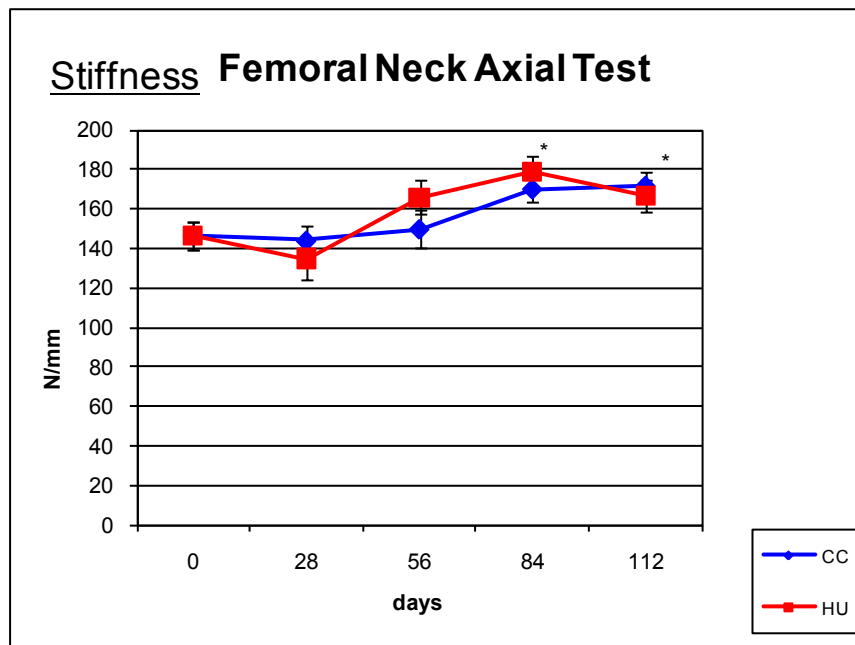
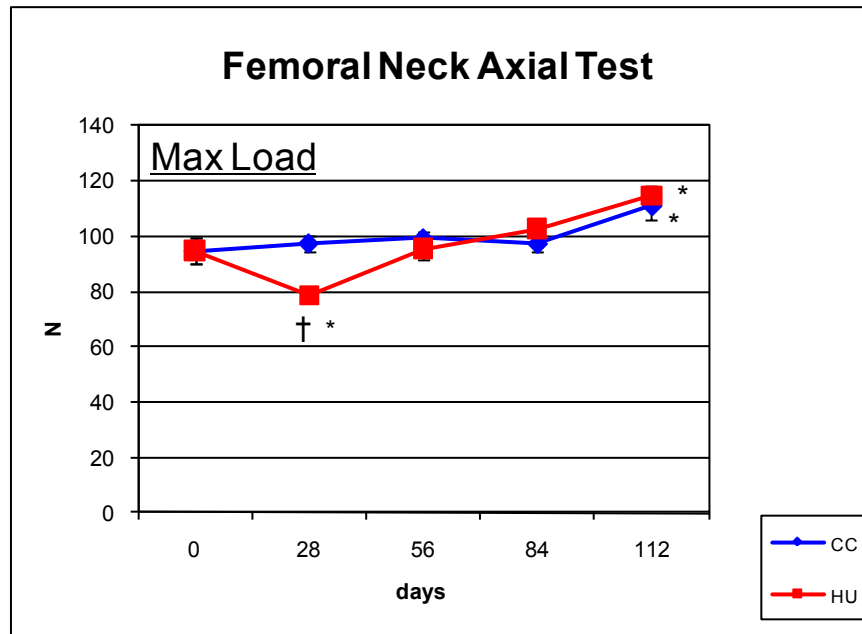


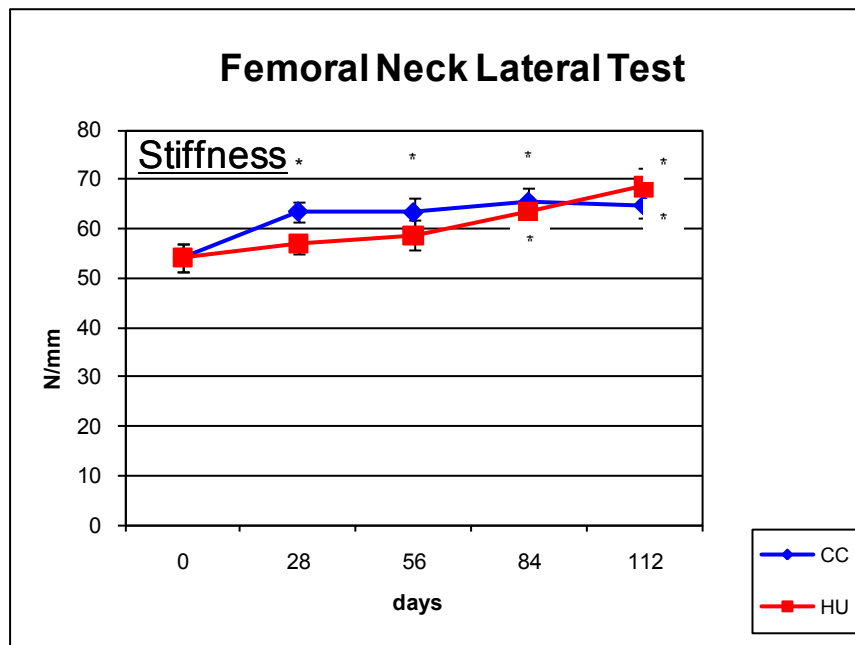
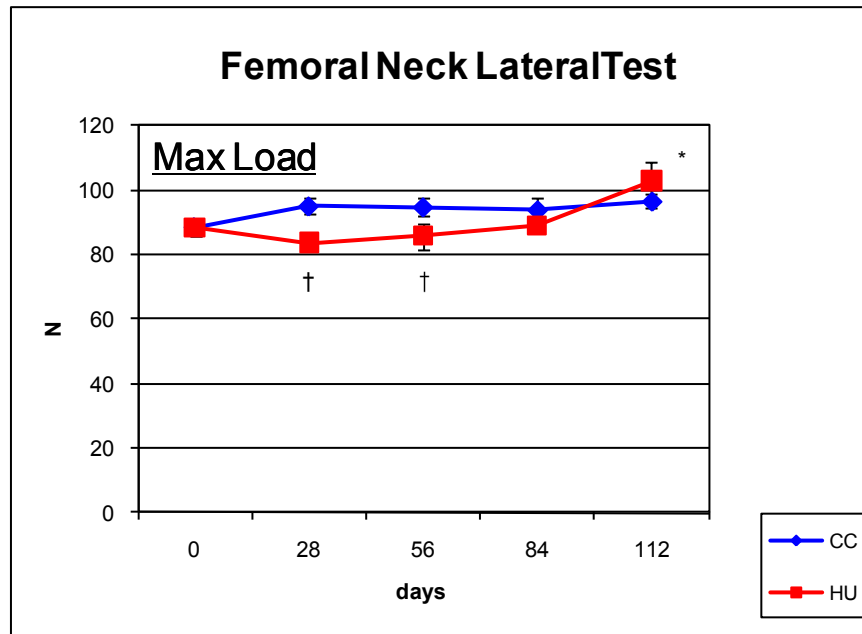




APPENDIX E

ABSOLUTE VALUE GRAPHS FOR AXIAL AND LATERAL TEST RESULTS





VITA

Name: Joshua Scott Kupke

Address: 3123 TAMU, College Station, TX 77843, C/O Dr. Harry Hogan

Email Address: josh.kupke@gmail.com

Education: B.S., Mechanical Engineering, University of Texas at Tyler, 2008
M.S., Biomedical Engineering, Texas A&M University, 2010